Zoological Journal of the Linnean Society, 2022, **196**, 316–345. With 14 figures.

Xenostrobus or *Vignadula* (Bivalvia: Mytilidae)? A taxonomic re-evaluation of small black mussels inhabiting the upper intertidal zone of the estuaries of Southeast Asia

KOH SIANG TAN[1,*], SAMUEL HUI MING TAN[2], KITITHORN SANPANICH[3], TEERAPONG DUANGDEE[4] and RENI AMBARWATI[5]

[1]*Tropical Marine Science Institute, National University of Singapore, Singapore*
[2]*School of Marine Sciences, University of Maine, Orono, ME, USA*
[3]*Institute of Marine Science, Burapha University, Chonburi, Thailand*
[4]*Faculty of Fisheries, Kasetsart University, Bangkok, Thailand*
[5]*Faculty of Mathematics and Natural Sciences, Universitas Negeri Surabaya, East Java, Indonesia*

Received 14 December 2021; revised 15 February 2022; accepted for publication 8 March 2022

The presence of small black mussels in the upper intertidal zone of estuarine seashores in Southeast Asia is often overlooked, despite their numerical dominance. Here, we clarify their species identities, taxonomy, geographical distributions and genetic relationships. Our molecular results suggest that three closely related species in East and Southeast Asia form a sister clade to Australian and New Zealand *Xenostrobus*. Given their distinctness, we resurrect the genus *Vignadula* to distinguish these two clades. *Vignadula atrata*, first described from Japan and type species of the genus, is confined to north-east Asia, whilst two other *Vignadula* species occur natively in Southeast Asia. Of these two species, one is found throughout Thailand, Malaysia, Singapore and Java. We show that this species corresponds to *Xenostrobus balani* and *Xenostrobus mangle* described from the Malacca Strait, which are genetically indistinguishable and here considered as one and the same species, ***Vignadula mangle* comb. nov.** The other species, ***Vignadula kuraburiensis* sp. nov.**, described in this study, has so far been found only in south-west Thailand. Members of *Vignadula* are, in turn, all clearly different from their closest morphological equivalent in Australia, *Xenostrobus pulex*. A new subfamily **Xenostrobinae** is proposed to accommodate the two genera *Xenostrobus* and *Vignadula*.

ADDITIONAL KEYWORDS: genetics – molecular phylogeny – Mollusca – morphological systematics – taxonomy.

INTRODUCTION

The mussel genus *Xenostrobus* Wilson, 1967 was originally proposed to delineate a few small to medium-sized modioline-like species distributed in southern Australia and New Zealand (Colgan & da Costa, 2013; Colgan *et al.*, 2020). They are distinguished from other mytilids in having their intestine loop along the right side of the animal instead of the left (Wilson, 1967). Four years later and without referring to *Xenostrobus*, Kuroda *et al.* (1971) proposed the genus *Vignadula* Kuroda & Habe in Kuroda *et al.* (1971) for the species *Mytilus atratus* Lischke, 1871, a small bluish-black intertidal mussel common in Japan, Korea and north-east China, based on conchological features. Wilson (1967) had earlier alluded to the similarities of the Japanese species and *Xenostrobus pulex* (Lamarck, 1819), a common intertidal mussel on the shores of southern Australia. Subsequently, Ockelmann (1983), when describing two *Xenostrobus* species (*Xenostrobus mangle* and *Xenostrobus balani*) from the Strait of Malacca, synonymized *Vignadula* with *Xenostrobus*. He attempted to distinguish these three Asian species based on anatomical details involving the shape of the guard papillae on the inner mantle lobes and the number of folds on labial palps.

*Corresponding author. E-mail: tmstanks@nus.edu.sg
[Version of record, published online 14 May 2022; http://zoobank.org/ urn:lsid:zoobank.org:pub:968C576E-4747-4586-9D48-C24C92741905]

The smooth, thin, edentate valves of *Xenostrobus* species have also misled workers in assigning them to the genus *Limnoperna* Rochebrune, 1882 (e.g. Habe, 1981; Beu, 2006; Huber, 2010: 546). Although this was shown not to be the case based on anatomical (Kimura *et al.*, 1999; Beu, 2012: 43) and genetic evidence (Colgan & da Costa, 2013), there is still uncertainty regarding whether *Limnoperna* is a monotypic genus (Sokolova *et al.*, 2021). The recent appearance of an Australian species, *Xenostrobus securis* (Lamarck, 1819), as an alien intertidal invasive in Japan (Kimura *et al.*, 1999; Iwasaki & Yamamoto, 2014), Korea (Park *et al.*, 2017) and Hong Kong (Morton & Leung, 2015) has led to further confusion over the identities of these mussels in East Asia. Despite being a common and often abundant filter-feeding component of the high intertidal fauna on continental shores of Southeast Asia, their systematic and phylogenetic position remains poorly defined. The aim of this study is to clarify and delineate the species of *Xenostrobus* and *Vignadula* present in East and Southeast Asia, using morphology and molecular sequences. Phylogenetic relationships between the species examined and their Australian (and New Zealand) relatives are also evaluated and discussed.

MATERIAL AND METHODS

Morphology

Mussel specimens were collected from various coastal localities across East and Southeast Asia, encompassing Japan, Taiwan, Hong Kong, Thailand, Malaysia, Singapore, Indonesia and Australia. Additional material was also examined, including types available for study in the following museums: Institut Royal des Sciences Naturelles de Belgique, Brussels, Belgium; Natural History Museum of Denmark, Copenhagen, Denmark; Muséum nationale de Histoire naturelle, Paris, France; Natural History Museum, London, UK; Phuket Marine Biological Center, Thailand; Zoological Reference Collection, Lee Kong Chian Natural History Museum, National University of Singapore; Tasmanian Museum and Art Gallery, Hobart, TAS, Australia; and Western Australian Museum, Perth, WA, Australia.

External features of intact and dead shells were noted, including the shell surface, periostracum, ligament, umbonal region and byssus. Where possible, living bivalves were placed in fresh seawater after collection and observed through a stereomicroscope to determine the shape and colour of the posterior inner mantle lobes and guard papillae. After preservation, shells of several specimens were either carefully cracked using a hand vice or their ligament and adductor muscles were cut to separate the valves before observations on their internal anatomy (labial palps, ctenidium, plicate gland, foot, byssal gland and mantle edges) were made. Others were preserved either in absolute ethanol for genetic sequencing/scanning electron microscopy or in 5% seawater formalin for further anatomical examination in the laboratory.

Shell microstructure was determined by examining cut or fractured shell surfaces under the scanning electron microscope (SEM). Cut surfaces were prepared by embedding clean, dry valves in epoxy resin blocks (Struer Epofix), which were then cut using a low-speed saw (Buehler IsoMet). The resulting block with the desired cut shell surface was ground and polished by hand over lapping film (3M) through a series of descending particle sizes to 3 µm grade, after which the polished surface was rinsed gently in distilled water and dried. A few drops of dilute 2% HCl v/v was then applied briefly (for ~5–10 s) to etch the cut surface before it was rinsed in distilled water, dried and sputter coated (JEOL 3000FC) with platinum for viewing by SEM (JEOL 6010/LVPlus). After breaking cleaned shells in the desired direction using a pair of scissors, the fractured surfaces were coated in a similar manner and viewed. Terminology of shell microstructure follows Carter (1990).

Molecular sequencing and analysis

DNA extraction

Specimens were stored in absolute ethanol until extraction. A part of the posterior adductor muscle tissue or the foot was extracted from these specimens, because extracting DNA from somatic tissue would reduce the problems associated with doubly uniparental inheritance present in the majority of mytilids (e.g. Garrido-Ramos *et al.*, 1998; Alves *et al.*, 2012; Robicheau *et al.*, 2016; Colgan, 2017). Tissue samples were processed using the DNeasy Blood & Tissue Kit (Qiagen) or the E.Z.N.A. Mollusc DNA Kit (Omega-Biotek) for particularly difficult specimens.

For both kits, dissected tissue was processed according to the manufacturer's instructions, with several modifications. Samples were incubated for extended periods of time until complete digestion, when necessary. To ensure maximum binding of extracted DNA to the spin columns, the initial lysate was passed through the column twice. Spin columns were washed with their associated wash buffers twice to remove contaminants. At the final elution step of pure genomic DNA, the eluant was allowed to incubate in the column at 50–70 °C (depending on kit recommendations) for 5 min to maximize the amount of DNA dissolved into the elution buffer. Extracted genomic DNA was quantified using a NanoDrop Lite (Thermo Scientific) spectrophotometer and a Qubit 3 fluorometer (Invitrogen). Aliquots of genomic DNA were taken and diluted to a concentration of 1 ng/µL for polymerase chain reaction (PCR). Concentrated genomic DNA was stored frozen at –20 °C for future use.

Polymerase chain reaction

Extracted genomic DNA was amplified through PCR in a T100 thermal cycler (Bio-Rad) or a ProFlex 3 × 32-well PCR System (Applied Biosystems). Five molecular markers, two mitochondrial (mt-*COI* and mt-16S) and three nuclear (ITS1, 28S D1R and *H3*), were targeted initially.

For the mitochondrial gene cytochrome *c* oxidase subunit I (mt-*COI*), a region ~700 bp in length was amplified using the universal primers LCO 1490: 5′-GGTCAACAAATCATAAAGATATTGG-3′ and HCO 2198: 5′-TAAACTTCAGGGTGACCAAAAAA TCA-3′ designed by Folmer *et al.* (1994), with the following thermal profile: initial denaturation at 95 °C for 3 min, followed by 35 cycles of denaturing at 95 °C for 1 min, annealing at 45.5 °C for 1 min and extension at 72 °C for 1.5 min; and a final extension at 72 °C for 7 min (Alves *et al.*, 2012). Should amplification with the Folmer primers fail, samples were amplified using the Colgan primers COXAF: 5′-CWAATCAYAAAGATATTGGAAC-3′ and COXAR: 5′-AATATAWACTTCWGGGTGACC-3′ (Colgan *et al.*, 2001), with the following thermal profile: initial denaturation at 95 °C for 5 min, followed by 35 cycles of denaturation at 94 °C for 3 min, annealing at 48 °C for 1 min and extension at 72 °C for 1 min; and a final extension at 72 °C for 7 min (Colgan *et al.*, 2003). Finally, should the Colgan primers fail, a 313 bp subset of the mt-*COI* gene was amplified with mICOIintF: 5′-GGWACWGGWTGAACWGTWTAYCCYCC-3′ and jgHCO2198: 5′-TAIACYTCIGGRTGICCRAARAA YCA-3′ (Leray *et al.*, 2013), with the following thermal profile: initial denaturation at min at 95 °C for 3 min; 35 cycles of denaturation at 95 °C for 1 min, annealing at 45 °C for 1 min and extension at 72 °C for 1 min; and a final extension at 72 °C for 3 min.

For the internal transcribed spacer 1 (ITS1), a region ~420 bp in length was amplified using ITS1A-sal: 5′-AAAAAGCTTTTGTACACACCGCCCGTCGC-3′ and ITS1B-sal: 5′-AGCTTGCTGCGTTCTTCATCGA-3′ (Pleyte *et al.*, 1992), with the following thermal profile: initial denaturation at 94 °C for 1.5 min, followed by 35 cycles of denaturation at 94 °C for 1.5 min, annealing at 65.2 °C for 1 min and extension at 72 °C for 2 min; and a final extension at 72 °C for 7 min (Pleyte *et al.*, 1992).

For the D1 expansion region of the 28S rRNA gene (D1R), a region ~350 bp in length was amplified using LSU5b: 5′-ACCCGCTGAAYTTAAGCA-3′ (McArthur & Koop,1999)andD1R:5′-AACTCTCTCMTTCARAGTTC-3′ (Colgan *et al.*, 2003), with the following thermal profile: initial denaturation at 95 °C for 5 min, 49 °C for 45 s and 72 °C for 1 min, followed by 34 cycles of denaturation at 95 °C for 30 s, annealing at 52 °C for 45 s, extension at 72 °C for 1 min; and a final cycle at 95 °C for 30 s, 52 °C for 45 s, extension at 72 °C for 5 min.

The histone H3 gene (*H3*) was amplified using H3af: 5′-ATGGCTCGTACCAAGCAGACVGC-3′ and H3ar: 5′-ATATCCTTRGGCATRATRGTGAC-3′, with the following thermal profile: initial denaturation at 94 °C for 3 min, followed by 30 cycles of denaturation at 95 °C for 30 s, annealing at 49 °C for 90 s and extension at 72 °C for 120 s; and a final extension at 72 °C for 5 min.

The 16S ribosomal RNA gene (16S) was amplified using 16SarL: 5′-CGCCTGTTTATCAAAAACAT-3′ and 16SbrH: 5′-CCGGTCTGAACTCAGATCACGT-3′, with the following thermal profile: initial denaturation at 94 °C for 5 min, followed by 35 cycles of denaturation at 94 °C for 30 s, annealing at 52 °C for 40 s and extension at 72 °C for 45 s; and a final extension at 72 °C for 5 min.

In general, each PCR contained 5 µL of 1 ng/µL DNA, 1 µL of each primer (10 µM) and 15 µL of GoTaq Green PCR Master Mix (Promega) or exTEN 2× PCR master mix (First Base) in a 30 µL reaction volume, with the remainder made up of nuclease-free water. Polymerase chain reaction additives (e.g. dimethyl sulfoxide or bovine serum albumin) were added as necessary for samples that were difficult to amplify.

Gel analysis, PCR purification and sequencing

The PCR products were analysed on a 1% agarose gel stained with SYBR Safe DNA Gel Stain or FloroSafe DNA Stain (First Base). Gel electrophoresis was carried out in standard 1× TAE buffer for 1 h, and gels were visualized using the Dark reader DR46B Transilluminator (Clare Chemical Research). Aliquots of amplified DNA were analysed on 1% agarose gel, with the remainder purified using the QIAquick PCR Purification Kit (Qiagen), should only the band of interest be present. Should non-specific amplification be present (e.g. primer-dimers), the remaining sample was run on a separate gel, and gel bands of appropriate sequence length and quantity were then purified using the QIAquick Gel Extraction Kit (Qiagen). Both methods were conducted following the manufacturer's instructions, with two exceptions. Initial samples were run through the spin columns twice to maximize DNA recovery, similarly for the eluate during the final elution step. Purified samples were sequenced bidirectionally using the BigDye Terminator sequencing system (Applied Biosystems) by First Base Asia (Singapore), using the same primers as the initial amplification steps mentioned above.

Data analysis

Sequences were filtered manually by trace scores, QV20+ (= total number of bases in the entire trace that have a basecaller Quality Value >=20 for Sanger sequencing) and contiguous read length in SEQUENCE SCANNER SOFTWARE 2 (Applied Biosystems). Sequences

were trimmed, edited and aligned in ALIVIEW (Larsson, 2014) using MUSCLE, with alignment being conducted with respect to codons for the protein-coding genes *COI* and *H3*. Owing to the low number of 16S sequences that successfully passed quality checks, the resultant 16S dataset was not used for the remainder of this analysis. Sequences were BLASTed against GenBank (using BLASTN) to confirm that they were Mytilidae, with *Xenostrobus* as the closest available relatives for putative *Xenostrobus* specimens.

All sequences obtained in this study were deposited in GenBank (National Center for Biotechnology Information) and are listed in the Supporting Information (Table S1). Reference sequences were obtained from GenBank, and these can also be found in the Supporting Information (Table S2).

All sequences were aligned, with mt-*COI* and *H3* sequences being checked for stop codons, in ALIVIEW (Larsson, 2014). All sequences for each barcode, including GenBank sequences, were checked for alignment before use in concatenated datasets. Sequences were concatenated using SEQUENCEMATRIX (Vaidya *et al.*, 2011). As part of initial data exploration, preliminary phylogenetic trees were generated in MEGA X (Kumar *et al.*, 2018) to determine whether there were any aberrant sequences attributable to doubly uniparental inheritance in *COI* or misidentification, because some concatenated sequences had to be constructed using sequences from different specimens and/or studies. Maximum likelihood (ML) trees using the Tamura–Nei model were generated for 10 000 bootstrap replicates, with 95% site coverage cut-off for gaps and missing data. Calculations of pairwise distances, between-group mean distances, net between-group mean distances and within-group mean distances were also conducted in MEGA X, with 1000 bootstrap replicates and rates as gamma distributed with invariant sites.

Given that single-gene trees resolved many important groups poorly, all the following analyses were conducted on the following datasets: mt-*COI* + ITS1 + 28S D1R + *H3*; mt-*COI* + 28S D1R + *H3*; and mt-*COI* + *H3*. Although mt-*COI* sequences were trimmed to the length of the shorter 313 bp mt-*COI* barcode to include as many samples as possible, a subset of these datasets with only full-length mt-*COI* sequences was also run. Non-mytilid pteriomorphs were used as the outgroups for all trees, except for the four-gene dataset, where Mytilidae of Clade B (*sensu* Morton *et al.*, 2020a; Clade 2 of Liu *et al.*, 2018 and Lee *et al*., 2019) were used instead.

Bayesian inference (BI) analyses were conducted in MRBAYES (Huelsenbeck & Ronquist, 2001) using the GTR substitution model partitioned by the different genes, with gamma-distributed rate variation across sites and a proportion of invariable sites (GTR+I). All parameters were unlinked between partitions. Two independent runs per dataset were conducted for a minimum of five million generations until posterior probability convergence as confirmed in TRACER v.1.7 (Rambaut *et al.*, 2018), with a sampling frequency of every 500 generations and a diagnostic frequency of every 5000 generations, with one cold and three heated chains and a relative burn-in fraction of 0.25.

Maximum likelihood analyses were conducted in IQ-TREE (Nguyen *et al.*, 2015) on the IQ-TREE web server (Trifinopoulos *et al.*, 2016). The software was allowed to determine substitution models automatically for each partition, with FreeRate heterogeneity. Ultrafast bootstrap analyses were conducted with 10 000 bootstrap replicates, in addition to SH-aLRt branch tests with 10 000 replicates. In addition to the above three datasets, an ML analysis was also conducted using full-length mt-*COI* sequences to examine further the position of the taxa (not shown) discussed in this paper with respect to other members of the Mytilidae.

All resultant trees were processed in FIGTREE v.1.4.4 (Rambaut, 2018), with tree annotations added in ADOBE ILLUSTRATOR. The concatenated dataset trees presented in this paper are Bayesian trees with ML data added onto branches sharing the same topology. The support values shown in the trees (e.g., 1/100) refer to BI/ML in that order.

INSTITUTIONAL ABBREVIATIONS

IRSN, Institut Royal des Sciences Naturelles de Belgique, Brussels, Belgium; MNHN, Muséum nationale de Histoire naturelle, Paris, France; NHM, Natural History Museum, London, UK; NHMD, Natural History Museum of Denmark (formerly Zoologisk Museum), University of Copenhagen, Denmark; NSMT, National Science Museum, Tsukuba, Japan; PMBC, Phuket Marine Biological Center, Thailand; TMAG, Tasmanian Museum and Art Gallery, Hobart, TAS, Australia; USNM, Smithsonian Institution, Washington, DC, USA; WAM, Western Australian Museum, Perth, WA, Australia; ZIN, Zoological Institute, Russian Academy of Sciences, St Petersburg, Russia; ZRC, Zoological Reference Collection, Lee Kong Chian Natural History Museum, National University of Singapore.

OTHER ABBREVIATIONS

LV, left valve; RV, right valve; SL, shell length.

RESULTS

MOLECULAR PHYLOGENY

A total of 68 *Xenostrobus* specimens from East and Southeast Asia were sequenced successfully. Concatenated phylogenetic trees (Figs 1–3) using

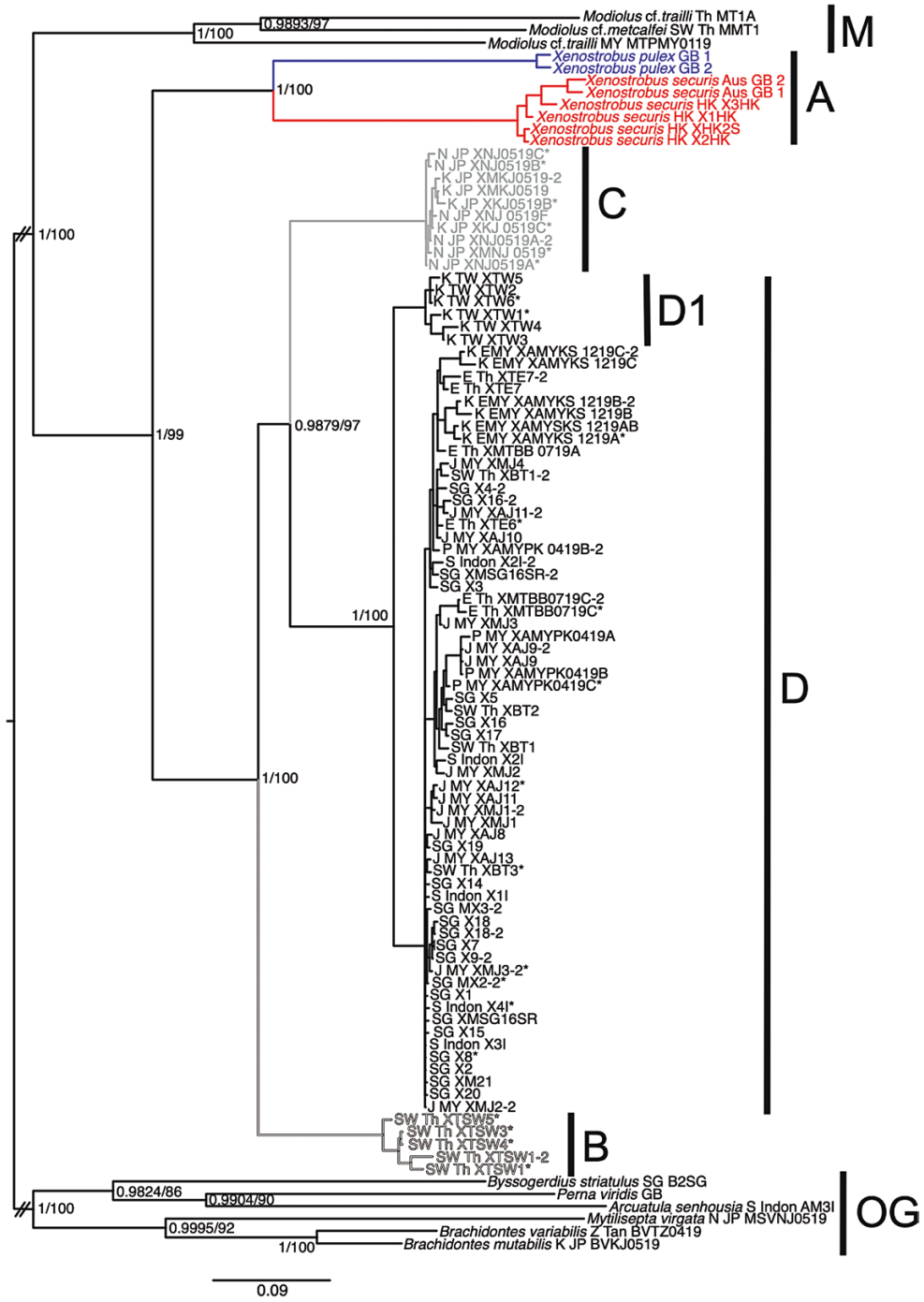

Figure 1. Concatenated four-gene Bayesian inference/maximum likelihood tree based on *COI*, ITS1, 28S D1R and *H3* sequences of *Xenostrobus* mussels from East Asia and Australasia. Both 313 bp and full-length *COI* barcodes were used in the analysis. In several cases (e.g. SG X18 and SG X18-2; XTSW1 and XTSW1-2), two sequences from the same individual were incorporated into the analysis. For readability, some nodes on the branch tips have been omitted and the lengths of some branches truncated (marked by a double slash). Sequence codes with asterisks were obtained from specimens shown in Figures 4–7. Line and text colours correspond to the colour scheme used to differentiate the geographical distributions of the species represented in the clades A, B, C and D. Sequence code abbreviations: E Th, Gulf of Thailand; FJP, Fukuoka, Japan; GB, GenBank; HK, Hong Kong; Indon, Indonesia; J MY, Johor, Malaysia; JP, Japan; K EMY, Kuching, East Malaysia; K JP, Kagoshima, Japan; K TW, Kinmen, Taiwan; N JP, Nagasaki, Japan; P MY, Perak, Malaysia; SG, Singapore; S Indon, Surabaya, Indonesia; SW Th, south-west Thailand; Th, Thailand; Z Tan, Zanzibar, Tanzania.

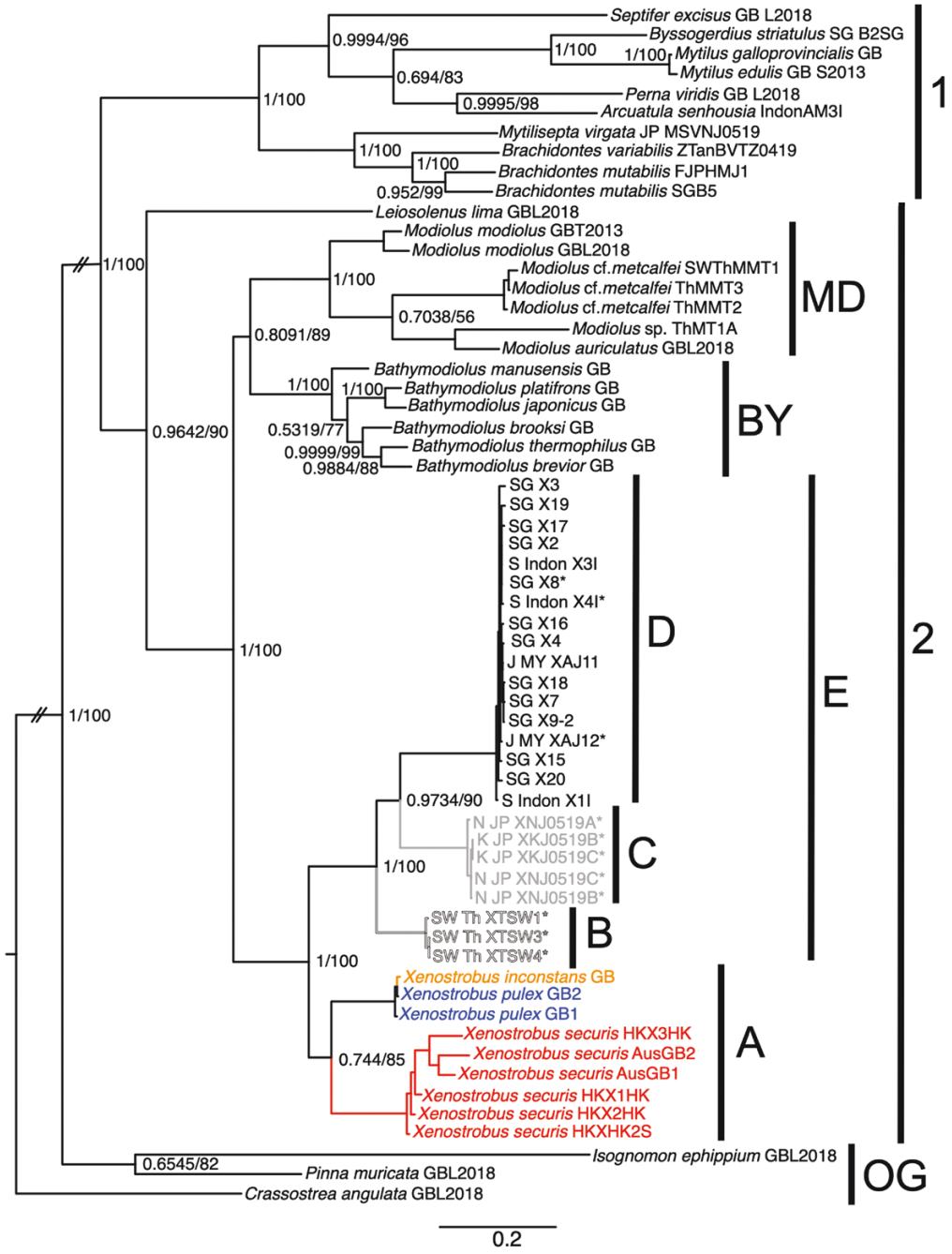

Figure 2. Concatenated three-gene Bayesian inference/maximum likelihood tree based on *COI*, 28S D1R and *H3* sequences of mussels from East Asia and Australasia, including additional sequences from GenBank. For readability, some nodes on the branch tips have been omitted and the lengths of some branches truncated (marked by a double slash). Sequence codes with asterisks were obtained from specimens shown in Figures 4–7. Line and text colours correspond to the colour scheme used to differentiate the geographical distributions of the species represented in the clades A, B, C and D. For an explanation of sequence code abbreviations, see legend to Figure 1.

four-gene (mt-*COI* + ITS1 + 28S D1R + *H3*), three-gene (mt-*COI* + 28S D1R + *H3*) and two-gene (mt-*COI* + *H3*) datasets all showed that *Xenostrobus* species formed a well-supported monophyletic group comprising Australian and New Zealand species (Clade A in Figs 1–3) together with East and Southeast Asian species (clades B + C + D in Figs 1–3; also Clade E in Fig. 2). Both clades A and E likewise

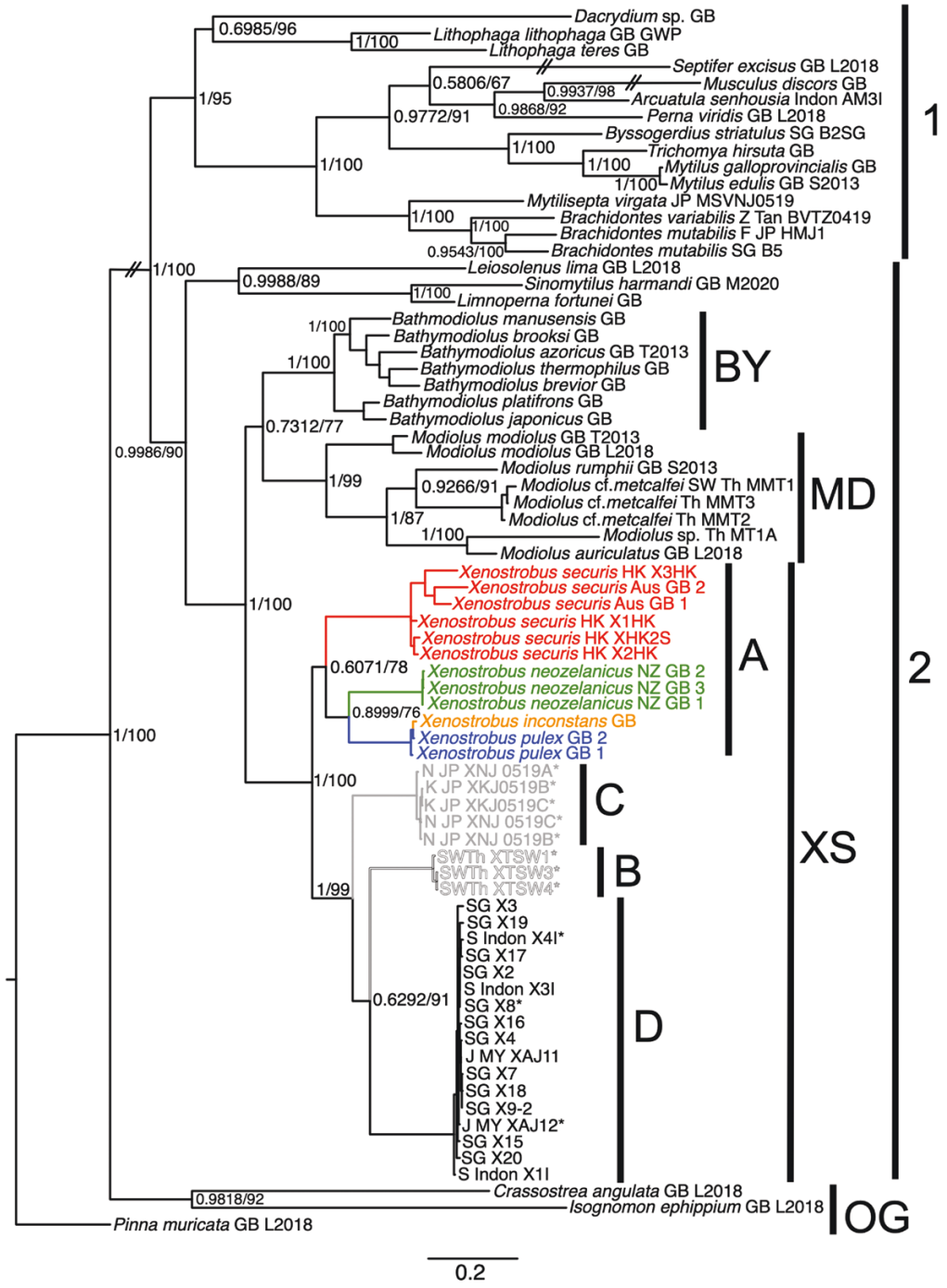

Figure 3. Concatenated two-gene Bayesian inference/maximum likelihood tree based on *COI* and *H3* sequences of mussels. For readability, some nodes on the branch tips have been omitted and the lengths of some branches truncated (marked by a double slash). Sequence codes with asterisks were obtained from specimens shown in Figures 4–7. Line and text colours correspond to the colour scheme used to differentiate the geographical distributions of the species represented in the clades A, B, C and D. For an explanation of sequence code abbreviations, see legend to Figure 1.

showed high support based on BI and ML methods. Overall tree topologies concerning these clades in the three concatenated trees were, in general, consistent with each other, except for the position of clades B and C in relationship to D in the four- and three-gene trees, which was inverted in the two-gene tree.

The *Xenostrobus* clade was sister to genera currently placed in the Bathymodiolinae (Clade BY)

and Modiolinae (Clade M in Fig. 1; MD in Figs 2, 3). Bootstrap estimates of average pairwise genetic distances between representative genera in the two subfamilies with those in the *Xenostrobus* clade ranged between 0.174 and 0.263 for mt-*COI*, 0.292–0.350 for ITS1, 0.0477–0.1215 for 28S D1R and 0.1030–0.1307 for *H3* (see Supporting Information, Tables S3–S6).

Within the *Xenostrobus* clade comprising East and Southeast Asian species, the four-gene tree (using both 313 bp and full-length fragments of *COI*) resolved four distinct groups: B, C, D and D1 (Fig. 1). Bootstrap estimates of average pairwise genetic distances between these putative species groups ranged between 0.1865 and 0.1989 for mt-*COI*, 0.1497–0.1716 for ITS1, 0.04405–0.01762 for 28S D1R and 0.0172–0.0370 for *H3* (see Supporting Information, Tables S7–S10). The average genetic distances between D1 (comprising specimens from Taiwan) and the rest of group D (from Thailand, Malaysia, Singapore and Indonesia) were 0.1251, 0.0200, 0.01322 and 0.0120 for mt-*COI*, ITS1, 28S D1R and *H3* genes, respectively.

These values, together with evidence based on morphology and distribution (see taxonomy section below for details), support: (1) the recognition of the *Xenostrobus* clade (XS in Fig. 3) as a distinct subfamily; and (2) the taxonomic division of the *Xenostrobus* clade into two genera corresponding to clades A and E (= B + C + D) in Figure 2. Clade A contains the type species of the genus *Xenostrobus*, *Xenostrobus inconstans* (Dunker, 1856), together with three other species, all of which are currently known to be native to Australia and/or New Zealand. Clade E contains the type species in the genus *Vignadula*, *Vignadula atrata* (Lischke, 1871) (Clade C), together with two other species (clades B and D, corresponding to *Vignadula mangle* and the new species *Vignadula kuraburiensis*; see Taxonomy section), all of which are restricted to East and Southeast Asia.

TAXONOMY

Order Mytilida

Superfamily Mytiloidea Rafinesque, 1815

Family Mytilidae Rafinesque, 1815

Xenostrobinae subfam. nov.

ZooBank registration: urn:lsid:zoobank.org:act:292A8499-1E98-4170-BB09-A1E5333FEB32

Diagnosis: Adult shell ≤ 40 mm in length, mytiliform to modioliform in outline, equivalve; shell surface generally dark purple or brown to black, generally smooth, often with closely set commarginal lines. Umbones subterminal or terminal. Shell interior iridescent, margins devoid of teeth. Ligament internal, resilial pits absent. Posterior adductor muscle scar confluent with single posterior byssal retractor muscle scar. Intestine makes a recurrent loop on the right side of the animal. Currently, Xenostrobinae comprises two genera and seven species distributed in East Asia and Australasia. All species are found in the mid- to upper littoral zone, and the majority live gregariously in or near estuaries.

Vignadula Kuroda & Habe in Kuroda *et al.*, 1971

Type species: Mytilus atratus Lischke, 1871a by original designation. Type locality: Nagasaki, Japan.

Diagnosis: Adult shell ≤ 15 mm. Posterior inner mantle edge of adult animal bears guard papillae. Distributed across East and Southeast Asia, from the Andaman Sea, Strait of Malacca, Gulf of Thailand, South China Sea, Yellow Sea and Sea of Japan.

Vignadula atrata (Lischke, 1871) (Figs 1–3, 8, 11, 12A, 13)

Mytilus atratus Lischke, 1871a: 44 and Lischke, 1871b: 146, pl. 10, figs 4, 4a, 5, 5b; type locality: Nagasaki, Japan. Holotype: *ZIN 2/111* (see Lutaenko & Chaban, 2016).

Modiola aterrima – Dall, 1871: 154 and pl. 14, fig. 13; type locality: Bay of Yeddo (Tokyo Bay). Holotype: *USNM 185505*.

Volsella atrata – Kuroda, 1932: 134, sp. 407.

Adula atrata – Habe & Kosuge, 1967: 127, pl. 47 fig. 10.

Xenostrobus atratus – Wilson, 1967: 284; – Ockelmann, 1983: 109–110, fig. 44 (graph); – Bernard *et al.*, 1993: 33–34 (in part); – Kimura, 1996: 97–100, figs 1–6; – Lutaenko *et al.*, 2019: 185 and pl. 9, figs I, J.

Hormomya atrata – Habe, 1968: 167–168, pl. 50, fig. 19.

Vignadula atrata – Kuroda *et al.*, 1971: 549 [in Japanese], 348 [in English], pl. 74, figs 5, 6; – Wang *et al.*, 2011: 87–88, figs. 3-71.

Xenostrobus atrata – Wang, 1997: 207–208, fig. 87; – Wang, 2004: p. 229, pl. 121E.

Diagnosis: Dark purplish blue to black mytiliform shells with terminal umbones; anterior half of ventral region often yellow to orange crossed by dark purple commarginal lines; animal without plicate gland; labial palps short, each palp bearing with ≤ 16 folds; mantle edge at posterior region of animal bears up to ten simple and/or branched guard papillae.

Material examined: **Japan**: Fukuoka-Amakusa (NSMT 49028); Kagoshima-Shoujigawa

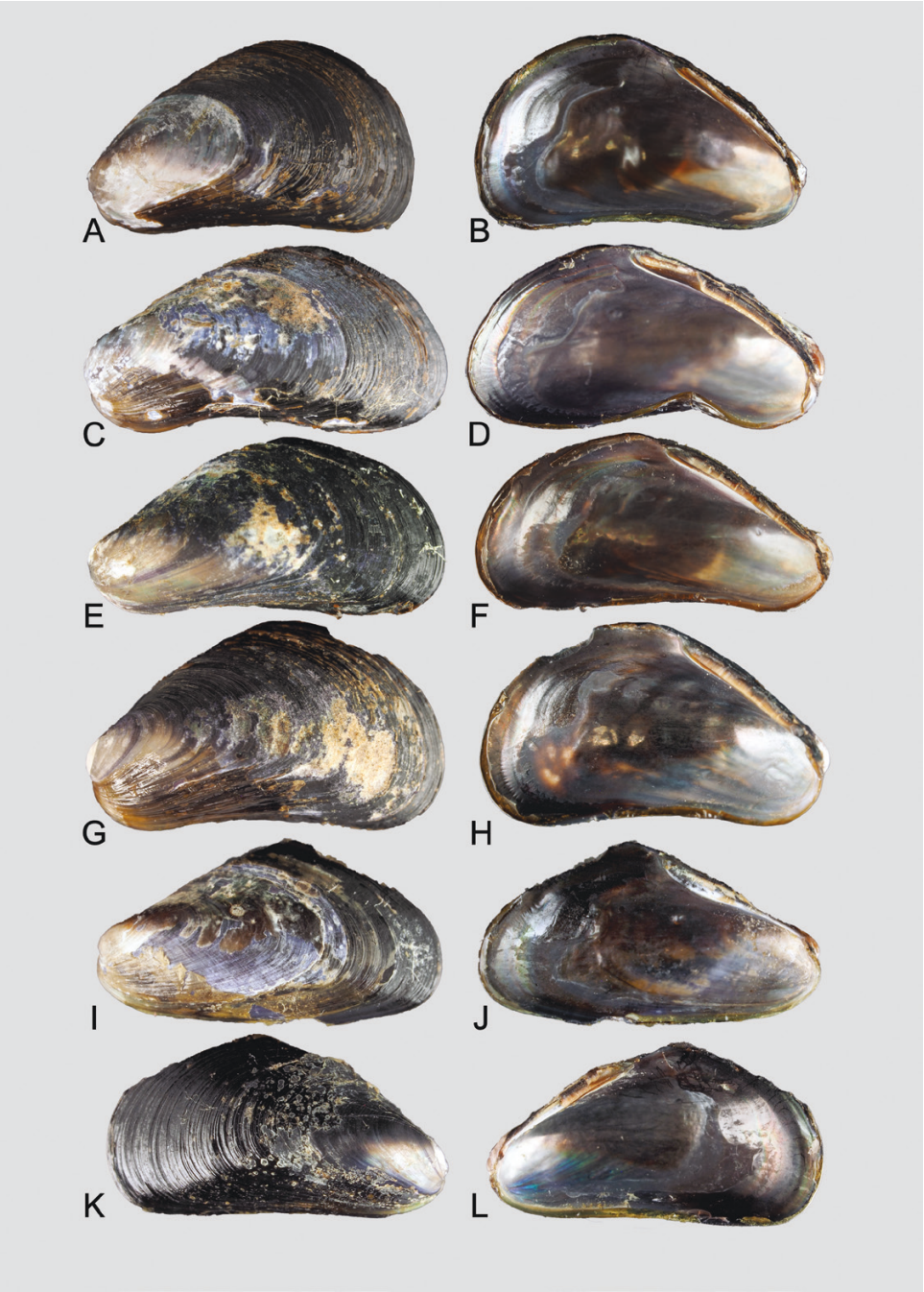

Figure 4. *Vignadula atrata* (Lischke, 1871). Sequenced specimens from Kyushu, Japan: A–H, Nagasaki; I–L, Kagoshima. A, B, XM NJ 0519; LV, SL = 11.2 mm (ZRC.MOL.24028). C, D, XNJ 0519A; LV, SL = 12.4 mm (ZRC.MOL.24029). E, F, XNJ 0519B; LV, SL = 10.6 mm (ZRC.MOL.24030). G, H, XNJ 0519C; LV, SL = 9.6 mm (ZRC.MOL.24031). I, J, XKJ 0519B; LV, SL = 8.0 mm (ZRC.MOL.24025). K, L, XKJ 0519C, SL = 6.6 mm (ZRC.MOL.24026). See also Clade C in Figures 1–3.

(ZRC.MOL.24027, 24916, 24917; PMBC 25330); Red Cross Hospital, Hirakawa (ZRC.MOL.24918, 24919); Ibusuki (ZRC.MOL.24920); Mie–Tsu (NSMT 58821); Miyagi-Fukuura Island (NSMT 44150); Nagasaki-Obama (ZRC.MOL.24921); Toishi-ko (ZRC.MOL.24922); Isomichimachi (ZRC.MOL.24923, 24924); Okayama-Kasaoka Bay (NSMT 49029). See also the Supporting Information (Table S1).

Shell: Variable in outline and shape, length ≤ 15 mm, mostly entirely dark purplish blue to black over the posterior two-thirds of length of valves, while the

anterior region is translucent yellow to orange crossed by fine dark purple commarginal lines where the periostracum is intact. Umbones terminal or in line with the edge of the anteroventral margin. Periostracal surface with fine, close-set commarginal lines free of byssal secretions. Ligament robust, long, stretching posteriorly from umbones to nearly half the length of the shell. Resilial pits are absent. At the region immediately below the umbones, there is a short, narrow shelf, but there are no hinge teeth anterior or posterior to the umbones. Likewise, there are no teeth posterior to the ligament. Interior of shell can generally be divided into a dark purplish brown dorsoposterior region and a lighter-coloured anteroventral region. Anterior region with prominent, oval anterior adductor muscle scar. Posterior adductor muscle scar continuous with byssal retractor muscle scars.

Shell microstructure: Shell generally comprises of two recognizable layers below the periostracum: a thin prismatic layer, under which a thick sheet nacreous layer is present. A thin, fibrous prismatic myostracum may be present within the sheet nacreous layer.

Anatomy: Inner mantle lobes forming the inhalant aperture are translucent orange-brown, with a high density of yellow subcutaneous pigment grains. The guard papillae are six to ten in number on each side. Each papilla is translucent white with small, white subcutaneous pigment grains. They may be simple or mixed with bi- or trifid papillae (Figs 8, 12A). The papillae all taper to a point when fully extended. They are highly contractile and if disturbed can be withdrawn completely to appear as folds or creases along the mantle edge. Juveniles < 2 mm SL do not possess guard papillae (Fig. 8A). Plicate organ is absent. Foot is yellowish white.

Two bundles of the posterior adductor muscle can (barely) be distinguished, and one is generally larger than the other, although their relative size varies between individuals. The posterior byssal retractor muscles are divided into two main bundles near the base of the foot. Of these, the anterior bundle is further divided into two or three bundles proximal to the shell. The pericardial complex is situated anterior to the posterior byssal retractor muscles (Category 2 of Morton, 2015a).

Labial palps vary in length according to shell size (see Theisen, 1982; Ockelmann, 1983), as does the number of folds (sorting ridges), which can range between five and 16 on each palp for SLs 4–12.5 mm (see Fig. 11).

Geographical distribution (Fig. 13): Korea (Jeju Island; see Lutaenko *et al.*, 2019), Japan and north-east China.

Taxonomic remarks: Mytilus atratus was first described from Nagasaki Bay, Japan by C. E. Lischke in 1871 (see Lutaenko & Chaban, 2016). Subsequent Japanese workers were undecided on its generic status, assigning the species variously to *Adula* H. Adams & A. Adams, 1857, *Hormomya* Mörch, 1853 and *Volsella* Scopoli, 1777 (see Kuroda, 1932; Habe & Kosuge, 1967; Habe, 1968). A century later, the species was assigned to *Vignadula* Kuroda & Habe in Kuroda *et al.* (1971), although Wilson (1967) recognized the possible connection between *V. atratus* and the Australian species of *Xenostrobus*. This was later followed up by Ockelmann (1983) and Lee & Morton (1985), who considered *Vignadula* a junior synonym of *Xenostrobus*. At about the same time, *Limnoperna fortunei kikuchii* Habe (1981) was described, which afterwards proved to be *X. securis* introduced from Australia and/or New Zealand (Kimura *et al.*, 1999). Kimura (1996) also described *X. atratus* in detail, and subsequently, Kimura *et al.* (1999) compared it with other congeners (see also Table 1). However, owing to its external resemblance to the tropical *V. mangle* (see below), the two species have sometimes been confused with each other (e.g. Wang, 1997; Liu *et al.*, 2011), particularly along the Chinese coast, where both species may occur and overlap in distribution.

VIGNADULA MANGLE (OCKELMANN, 1983) COMB. NOV.

(FIGS 1–3, 5, 6, 9–11, 12B, 13)

Xenostrobus mangle Ockelmann, 1983: 104–106, figs 32–35, 38, 40, 43, 44; type locality: Jeram, Kuala Selangor, west coast of Malaysia. Holotype *NHMD 77043* (*BIV-001811*): missing; NHMD 916051: 57 paratypes (27 intact individuals and 30 valves).

Xenostrobus balani – Ockelmann, 1983: 107–111, figs 36, 37, 39, 41, 43–45; type locality: mangrove of Ao Nam Bor, Phuket, Thailand. Holotype missing. NHMD 915909: five paratypes; PMBC 3104: three paratypes (Aungtonya *et al.*, 1999).

Xenostrobus aratus (Dunker, 1856) – Nguyen, 2001: 417 (not *aratus* [sic]).

Xenostrobus atrata (Lischke, 1871) – Lee & Morton, 1985: 54–55, pl. 2A (not *atrata*); – Wang, 1997 (in part): 208, fig. 87 (not *atrata*).

Xenostrobus atratus – Bernard *et al.*, 1993: 33–34 (in part); – Kurozumi, 2000: 429–430 and pl. 429, fig. 6 (not *atratus*?); – Kurozumi, 2017: 1173 and pl. 472, fig. 9 (not *atratus*?).

Xenostrobus sp. – Ng & Sivasothi, 1999: 119, fig.

Diagnosis: Dark purple to black mytiliform shells with a trapezoid outline and mostly subterminal umbones; anterior half of ventral region often yellow to orange crossed by dark purple commarginal lines; animal with inner and outer plicate glands; labial palps long, each palp with ≤ 60 folds; mantle edge at posterior region of animal bears ≤ 14 simple and/or branched guard papillae.

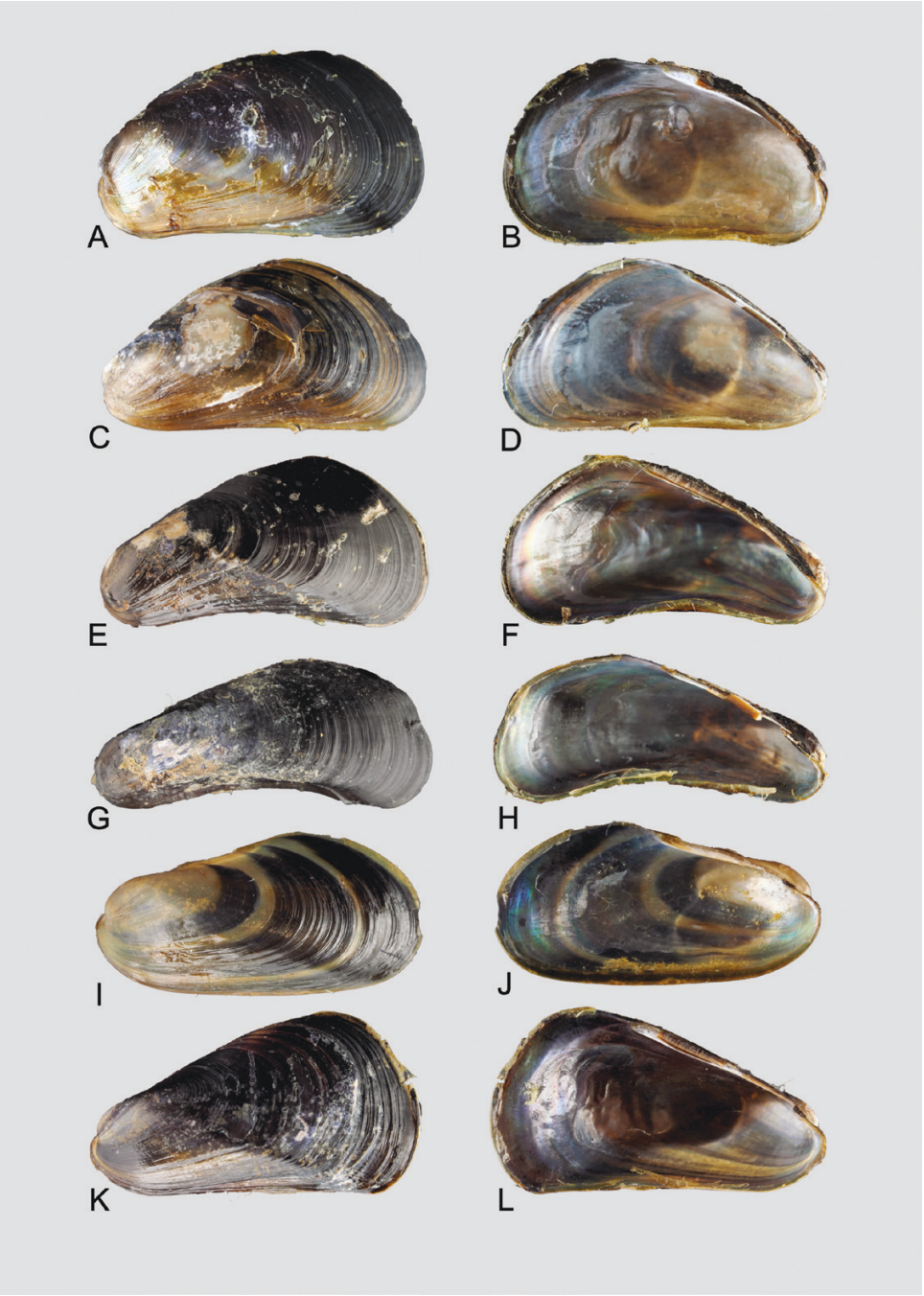

Figure 5. *Vignadula mangle* (Ockelmann, 1983) comb. nov. Selected sequenced specimens from Indonesia (A, B), Malaysia (C, D, I–L) and Singapore (E–H). A, B, X4I, Surabaya, E. Java; LV, SL = 9.9 mm (ZRC.MOL.24045). C, D, XA MYKS 1219A, Kampong Bako, Sarawak (Borneo); LV, SL = 12.8 mm (ZRC.MOL.24021). E, F, X8, Punggol Point; LV, SL = 10.1 mm (ZRC.MOL.24054). G, H, MX2, Sembawang Park; LV, SL = 14.8 mm (ZRC.MOL.24046). I, J, XAJ 12, Sungei Punggur, Johor (Malacca Strait); LV, SL = 6.8 mm (ZRC.MOL.24015). K, L, XMJ 3, Sungei Punggur, Johor (Malacca Strait); LV, SL = 10.9 mm (ZRC.MOL.24019). See also Clade D in Figures 1–3.

Nomenclature: Ockelmann (1983) designated and illustrated the holotype of *X. mangle* but did not isolate the specimen from amongst some 27 intact individuals and 30 valves designated paratypes at NHMD. However, none of the paratype shells in NHMD matches the overall appearance and dimensions of the holotype provided by Ockelmann. In the case of *X. balani*, the holotype specimen is missing from the vial marked holotype in the NHMD

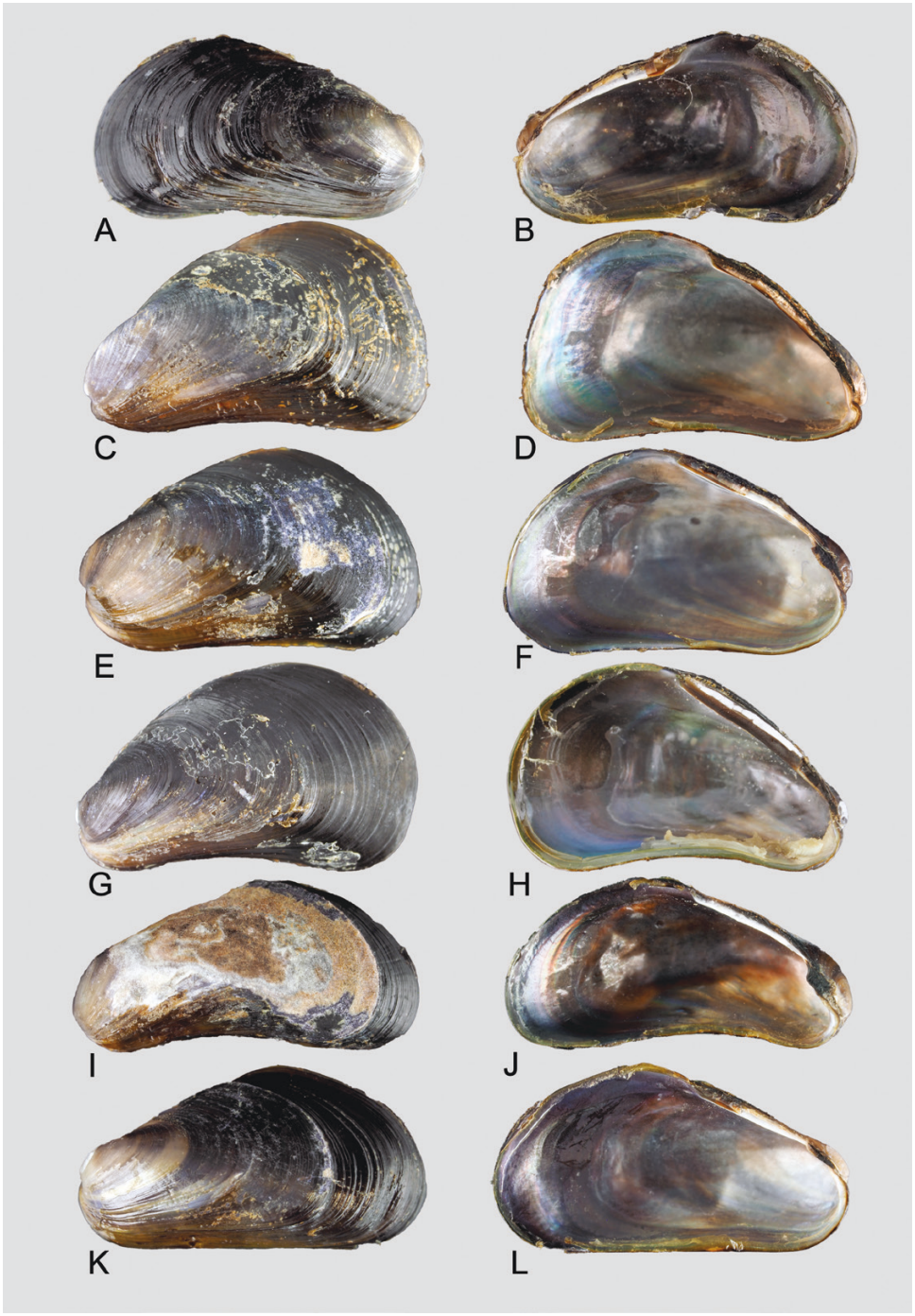

Figure 6. *Vignadula mangle* (Ockelmann, 1983) comb. nov. Selected sequenced specimens from Malaysia (A, B), Thailand (C–H) and Taiwan (I–L). A, B, XA MYPK 0419C, Lumut, Perak (Malacca Strait); RV, SL = 6.2 mm (ZRC.MOL.24041). C, D, XBT3, Pak Meng, Trang Province, Thailand (Andaman Sea); LV, SL = 11.9 mm (ZRC.MOL.24067). E, F, XTE6, Hua Hin, Prachuap Khiri Khan Province (Gulf of Thailand); LV, SL = 10.1 mm (ZRC.MOL.24004). G, H, XM TBB 0719C, Bangsaen Beach, Chonburi Province (Gulf of Thailand); LV, SL = 9.7 mm (ZRC.MOL.24007). I, J, XTW1, Kinmen, Taiwan; LV, SL = 9.2 mm (ZRC.MOL.24033). K, L, XTW6, Kinmen, Taiwan; LV, SL = 9.5 mm (ZRC.MOL.24038). See also Clade D in Figures 1–3.

collection (T. Schiøtte, pers. comms.). The ten separated valves (referable to five individuals) in the paratype lot at NHMD all do not match exactly the holotype dimensions given by Ockelmann (1983). Nevertheless, these irregularities do not affect the conclusions reached in this study.

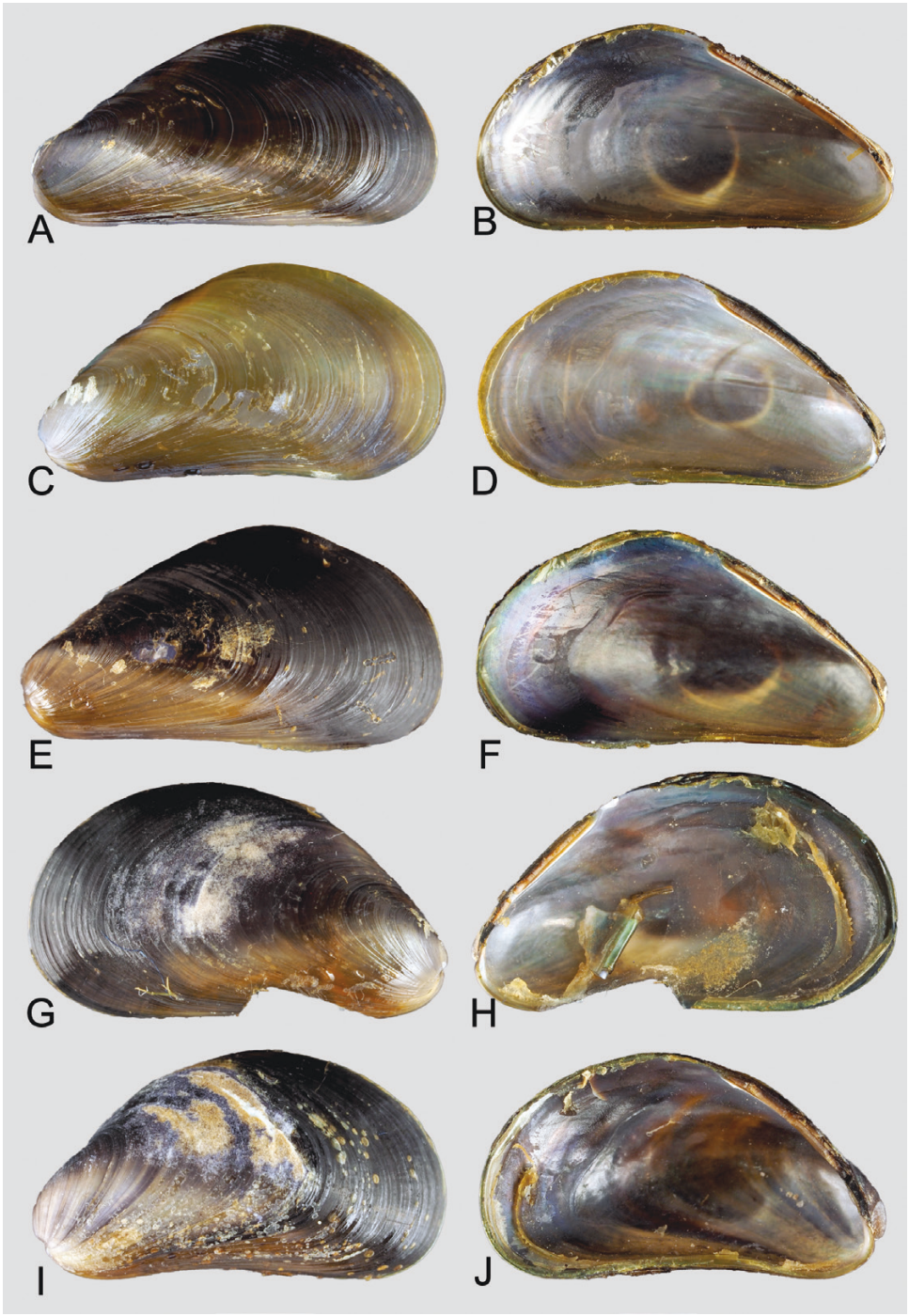

Figure 7. *Vignadula kuraburiensis* sp. nov. Sequenced specimens from western Thailand: A–H, Ban Thung La Ong in Kuraburi District, Phang-nga Province; I, J, Bang Ben Bay, Laem Son National Park, Kapoe District, Ranong Province. A, B, XTSW1; LV, SL = 12.8 mm (holotype, *PMBC 25290*). C, D, XTSW2; LV, SL = 13.2 mm (paratype, PMBC 25291). E, F, XTSW3; LV, SL = 12.3 mm (paratype ZRC.MOL.24068). G, H, XTSW4; RV (anterior half of ventral edge partially broken), SL = 11.5 mm (ZRC.MOL.24069). I, J, XTSW5; LV, SL = 9.0 mm (ZRC.MOL.24070). See also Clade B in Figures 1–3.

Material examined: **Taiwan**: Husia, Kinmen (off Xiamen, China) (ZRC.MOL.24925); **Vietnam:** Sung Sot Cave, Ile de la Surprise off Cat Ba Island, Gulf of Tonkin (ZRC.MOL.24926); **Thailand**: Andaman Sea–Pak Bara, Satun (ZRC.MOL.24927, 24928; PMBC 25331); Ko Talibong, Trang (ZRC.MOL.24929; PMBC 25332); Pak

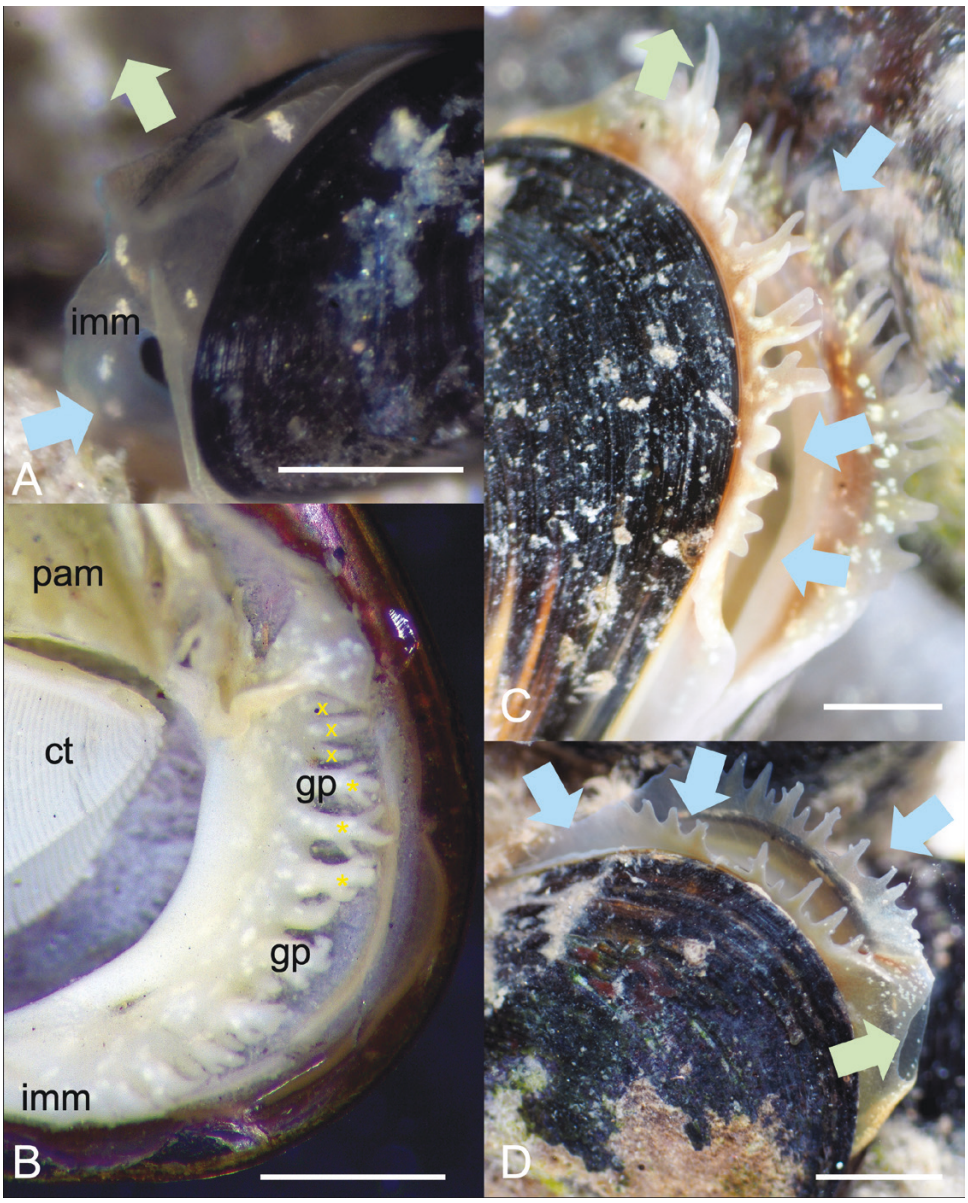

Figure 8. *Vignadula atrata* (Lischke, 1871). A, posterior region of living juvenile with extended mantle margins (imm) devoid of guard papillae. Blue and green arrows depict the direction of inhalant and exhalant currents. Scale bar: 500 µm. B, posterior region of ethanol-preserved sequenced individual XNJ 0519B, with left valve removed to show posterior end of ctenidium (ct), mixture of simple (marked by yellow crosses) and branched (yellow asterisks) guard papillae (gp) along the inner mantle margin (imm) and posterior adductor muscle (pam). Scale bar: 1 mm. C, living individual with numerous simple and branched guard papillae. Scale bar: ~500 µm. D, living individual with mostly simple guard papillae. Note the well-formed exhalant siphon. Scale bar: ~1 mm. A, Kagoshima, Japan. B–D, Nagasaki, Japan.

Meng, Trang (ZRC.MOL.24067); Phuket, Ao Nam Bor (NHMD 915909; PMBC 3104, 3732); Gulf of Thailand-Pranburi (ZRC.MOL.24930; PMBC 25333); Hua Hin (ZRC.MOL.24004, 24005); Bangsaen (ZRC.MOL.24931, 24932; PMBC 25334); Pattaya (ZRC.MOL.24006); Laem Hin, Trat (ZRC.MOL.24933, 24934; PMBC 25335, 25336); **Malaysia**: Johor west coast-Sungei Punggur (ZRC.MOL.24935); Sungei Lurus (ZRC.MOL.24936); Pontian Kechil (ZRC.MOL.24937); Minyak Beku (ZRC.MOL.24938); Selangor-Jeram (*NHMD 77043*); Perak-Teluk Batik, Lumut (ZRC.MOL.24039, 24939); Teluk Senangin (ZRC.MOL.24940); Kedah-Tanjung Jaga (ZRC.MOL.24941); Penang-Gertak Sanggul (ZRC.MOL.24942); Batu Ferringhi (ZRC.MOL.24943); Sarawak-Santubong (ZRC.MOL.24944); Kampung Bako, north of Kuching (ZRC.MOL.24022, 24945);

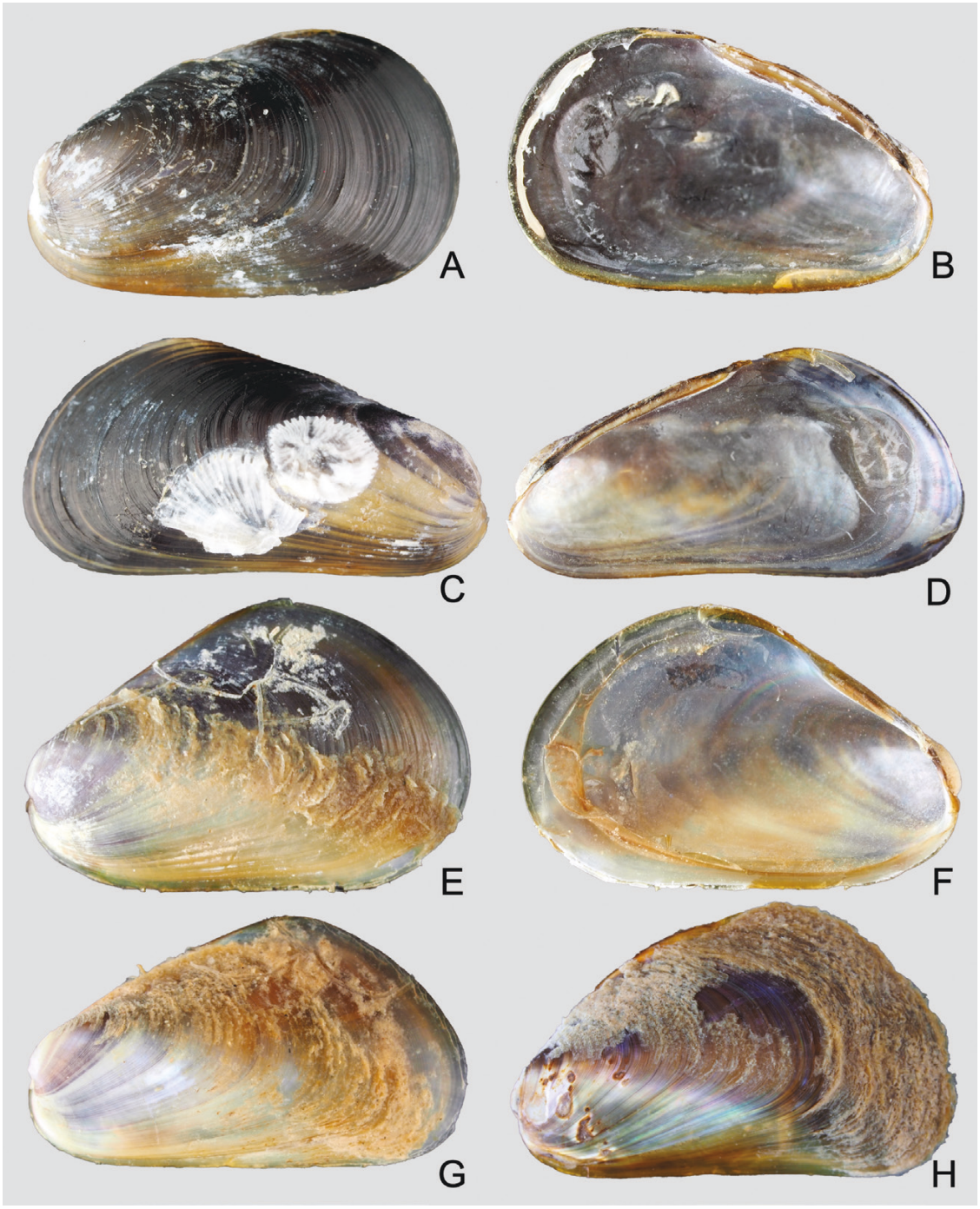

Figure 9. Type material of *Vignadula mangle* comb. nov. and *Vignadula balani*. A–D, *Xenostrobus mangle* Ockelmann, 1983 paratypes NHMD 916051 Jeram, Selangor, peninsular Malaysia. A, B, SL = 8.2 mm. C, D, SL = 11.0 mm. E–H, *Xenostrobus balani* Ockelmann, 1983 paratypes NHMD 915909 Phuket, Thailand. E, F, SL = 6.4 mm. G, LV, SL = 7.2 mm. H, LV, SL = 8.5 mm.

Singapore: Raffles Marina (ZRC.MOL.24946); Tengeh Buoy (ZRC.MOL.24947); Sarimbun (ZRC.MOL.24064); Sungei Buloh (ZRC.MOL.24948, 24949); Kranji (ZRC.MOL.24950); Sembawang Park (ZRC.MOL.24951); Tanjong Irau, Sembawang (ZRC.MOL.24952, 24953); Punggol Point (ZRC.MOL.24053); Changi Village (ZRC.MOL.24056, 24057, 24058); Paku Buoy (ZRC.MOL.24954); Siglap Canal (ZRC.MOL.24955);

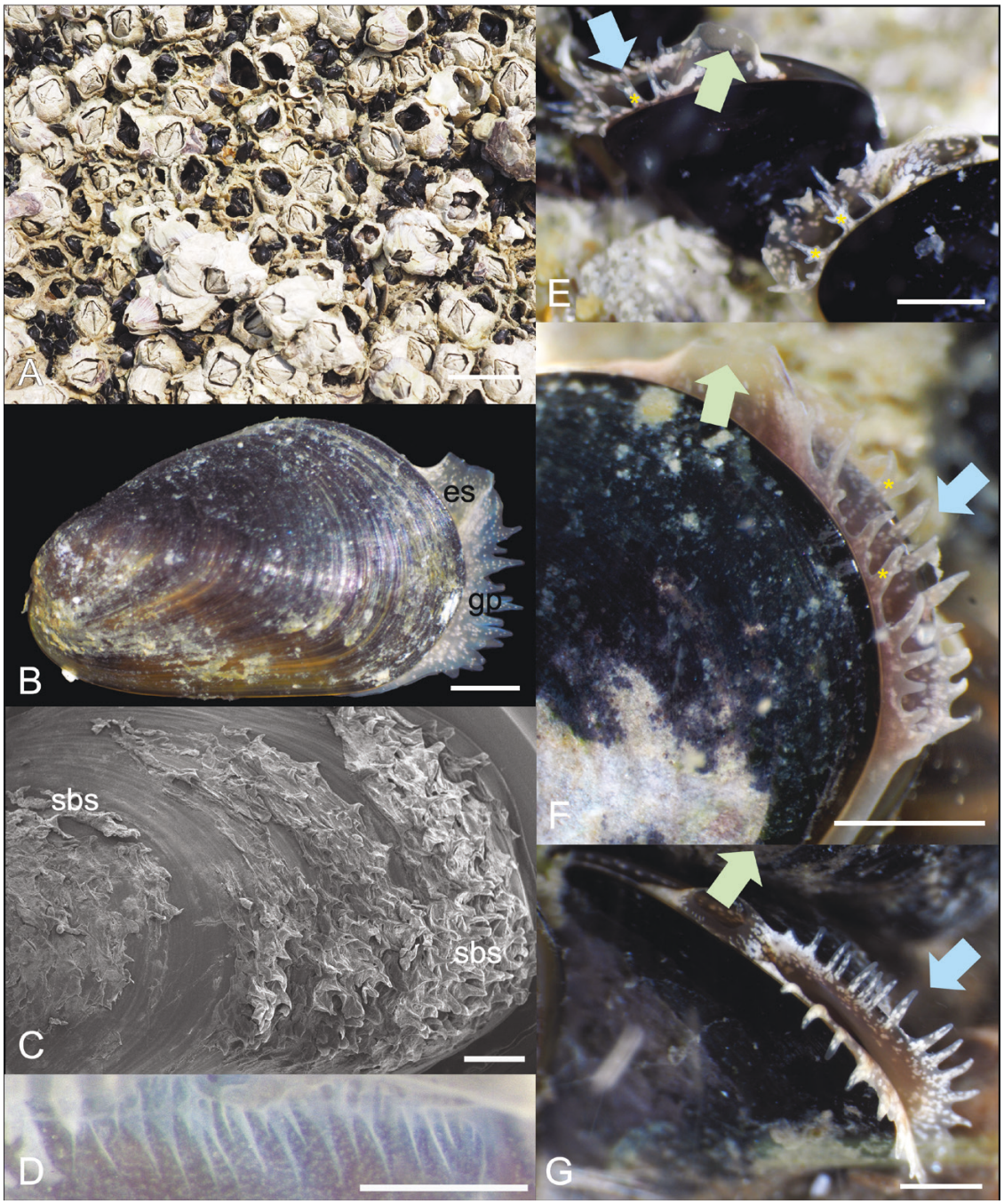

Figure 10. *Vignadula mangle* (Ockelmann, 1983) comb. nov. A, numerous individuals amongst barnacles (*Amphibalanus amphitrite* (Darwin, 1854)) on an intertidal rocky shore at Teluk Senangin, Perak, Malaysia. Scale bar: 1 cm. B, intact living individual seen from its left, with extended inhalant (inner mantle lobes bearing simple guard papillae, gp) and exhalant (es) siphons. Scale bar: 1 mm. C, surface of posterior half of left valve (SL = 8.0 mm; specimen collected from Sembawang, Singapore) with 'special byssus secretions' (sbs), or commarginal series of thickenings or blunt serrations, *sensu* Ockelmann (1983). Scale bar: 500 µm. D, outer plicate gland, after removal of ctenidium. Scale bar: 1 mm. E–G, detail of the posterior region of living individuals, showing simple and branched (yellow asterisks) guard papillae. Both types of papillae can occur in the same individual, as shown in E and F. Blue and green arrows depict the direction of inhalant and exhalant currents. Scale bars: 1 mm. D, Hat Yao jetty, Trang, Gulf of Thailand. E, Teluk Batik, Lumut, Perak. B, F, G, Bangsaen Beach, Chonburi, Gulf of Thailand.

Indonesia: Surabaya, East Java (ZRC.MOL.24956). See also the Supporting Information (Table S1).

Shell: Variable in outline and shape, length ≤ 15 mm, thin, overall outline trapezoid; the blunt, inflated anterior region is defined by distinct umbonal and anteroventral extensions, while the posterior region is broad and flat. Surface mostly entirely purplish black over the posterior two-thirds of length of valves, while the anteroventral region is translucent yellow to orange crossed by fine dark purple, closely set commarginal lines where the periostracum is intact. Umbones in most cases subterminal to the distinct, rounded anteroventral margin. Shell interior iridescent, margins devoid of teeth. Ligament narrow, smooth without teeth; resilial pits absent.

Shell microstructure: Shell generally comprises two layers below the periostracum: a thin prismatic layer, under which a thick, sheet nacreous layer is present. A thin, fibrous prismatic myostracum may be present within the sheet nacreous layer.

Anatomy: Up to 14 simple or branched (bifid, trifid or quadrifid) guard papillae (Figs 10E–G, 12B) along one edge of inner mantle forming inhalant siphon. Papillae translucent pink to white, with small white subcutaneous pigment grains. Smaller individuals tend to have fewer guard papillae, which are invariably simple (not branched). In individuals with SLs < 2–3 mm, the inner mantle edge forming the inhalant aperture is generally entire, with no papillae. Foot yellowish white, vermiform.

Two adjacent bundles of the posterior adductor muscle can be distinguished. One is generally larger than the other, although their relative size varies between individuals. Posterior byssal retractor muscles are split into two bundles near base of foot, but the anterior bundle is further divided into two or three subbundles towards the shell (as observed on animal, but the muscle scars on the valves do not reflect this separation). Pericardium lies anterior to the posterior byssal retractor muscle complex (Category 2 of Morton, 2015a).

Plicate organ (organ of Sabatier; Fig. 10D) present on the roofs of the suprabranchial chamber, along length of bases of outer and inner demibranchs on the left and right sides of the animal. Labial palps vary in length according to shell size (see Theisen, 1982; Ockelmann, 1983), as does the number of folds (sorting ridges), which can range between nine and 55 for SLs 2–13 mm (Fig. 11).

Ecology: Found singly or in small groups of two to four individuals inside empty barnacle (often *Balanus amphitrite* Darwin, 1854) shells together with Acari, collembolans and the estuarine bryozoan *Sundanella sibogae* (Harmer, 1915) in the upper- to mid-intertidal zone of estuaries and mangroves. They can also be found in large numbers clustered together over rocks or concrete surfaces in the intertidal zone in estuaries. However, they can also occur subtidally, as observed by Madin *et al.* (2009) on recruitment nylon net panels placed vertically in floating net cages. Leh *et al.* (2012) showed that *V. mangle*, together with other bivalves [*Anadara granosa* (Linnaeus, 1758) and *Placuna* sp.] composed ≤ 50% of the diet of the eel catfish *Plotosus canius* Hamilton, 1822 along the west coast of peninsular Malaysia.

Geographical distribution (Fig. 13): Kinmen (off Xiamen, China) southwards to the Gulf of Thailand, Malaysia, Singapore, Strait of Malacca and the Andaman Sea; Borneo and Java. Curiously, there were no records of *V. mangle* or *V. atrata* from the main island of Taiwan itself in the National Museum of Natural Science in Taichung, Taiwan.

Taxonomic remarks: Ockelmann (1983) described two *Xenostrobus* species, *X. mangle* and *X. balani*, from Jeram in the Malacca Strait and Phuket Island adjoining the Andaman Sea, respectively. They were distinguished chiefly based on the sizes of their shells and labial palps, which are both relatively larger in *X. mangle* compared with *X. balani* as diagnosed by Ockelmann (Table 1). Also, size asymmetry of the two bundles making up the posterior adductor muscle was noticed to be more marked in *X. balani* than in *X. mangle*. 'Special byssal secretions' (Fig. 10C) on the shell surface of *X. balani* (see paratypes: Fig. 9E, G, H) that comprise commarginal thickenings or serrations are weak or absent in *X. mangle*, according to Ockelmann (1983). In addition, the byssal gland of *X. balani* is branching and penetrates deeply into the visceral mass, in contrast to the condensed, non-branching gland in *X. mangle* (for a summary of characters, see Table 1).

In this study, we collected, examined and sequenced material from across a wide geographical range encompassing locations in the East China Sea, South China Sea, Malacca Strait, the Andaman Sea and Java Sea. Our observations suggest the existence of a continuum of morphological character states, instead of disjunct states that Ockelmann used to distinguish *X. mangle* and *X. balani*. This is particularly the case for the relative sizes of two muscle bundles of the posterior adductor muscle, the presence or absence of byssal secretions on the valves, the condition of the byssal gland and the number of folds on the labial palps. Nevertheless, the existence of two phenotypes [i.e. individuals having labial palps that are either

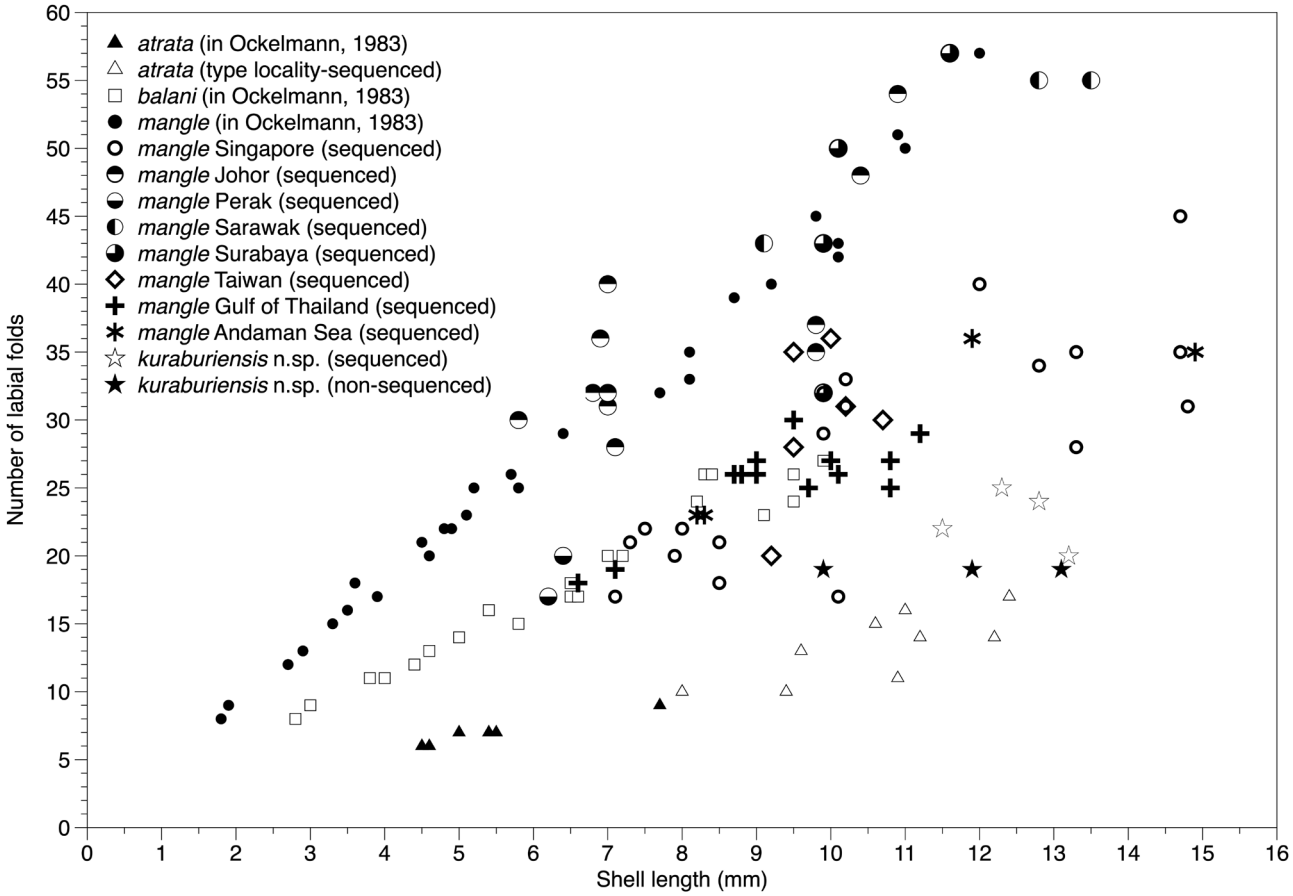

Figure 11. Relationship between shell size and number of folds observed on the labial palps of four *Vignadula* species from East and Southeast Asia. Data from Ockelmann (1983) for *Vignadula atrata*, *Vignadula balani* and *Vignadula mangle* are indicated separately. Apart from data points based on the study by Ockelmann (1983) and three individuals of *Vignadula kuraburiensis* sp. nov., all are referable to genetically sequenced individuals based on this study.

short or long (corresponding to a smaller or larger number of folds) as shown by Ockelmann (1983)] appears to be real (see Fig. 11) amongst the otherwise genetically indistinguishable individuals we observed in this study. Interestingly, the two phenotypes seem to be location specific; for instance, all individuals collected in this study and sequenced from Singapore, Gulf of Thailand, Andaman Sea and Taiwan had small labial palps, whereas those from localities in Johor, Sarawak (Borneo) and Surabaya in Java had large labial palps. However, they all shared the apomorphy of having a plicate gland along the bases of the outer and inner demibranchs on both left and right sides of the animal.

Ockelmann (1983) also observed that 'almost all' *X. balani* were found singly in empty barnacle shells, whereas *X. mangle* were '…living together with *Balanus amphitrite*…' and '…were found byssally attached to their congeners' valves', occurring '…gregariously as members of the epifauna on mangrove roots and on stony substrata'. Our observations showed that *X. mangle* can indeed be found inside barnacle shells, not only singly, but gregariously in groups of up to several individuals depending on the size of the empty barnacle shells. These tended to be smaller individuals of *X. mangle* possessing largely intact 'special byssal secretions' (Fig. 10C), possibly because of the sheltered nature of the microhabitat, which is also used by other organisms, such as mites, collembolans and the high shore bryozoan *Sundanella sibogae*. Conversely, Ockelmann (1983) stated that many individuals of *X. mangle* living outside barnacle shells had live barnacles attached to their shells, which he attributed to the absence of 'special byssal secretions'. We also observed some individuals fouled by barnacles, but these were not restricted to those living outside dead barnacle shells. Hence, based on these field observations, considered together with their similar morphology and genetic composition, we conclude that *X. balani* and *X. mangle* are one and the same species.

Table 1. Comparison of *Vignadula* species with *Xenostrobus pulex*

Character	*Vignadula atrata*	*Vignadula balani*	*Vignadula mangle* comb. nov.	*Vignadula kuraburiensis* sp. nov.	*Xenostrobus pulex*
Guard papillae around inhalant opening	Non-branching papillae; few branching near exhalant siphon and mostly non-branching papillae (total 9 papillae on each side on inhalant siphon); 9–12 simple or branching papillae that are largest midway between exhalant siphon and ventral extremity of inhalant siphon	Simple, small	Simple, large, increasing in size towards exhalant siphon; 4–12 simple or branching papillae that are largest midway between exhalant siphon and ventral extremity of inhalant siphon	Simple, small, numerous (≤ 14 papillae)	Branching papillae; simple or branched, small and numerous (12 in SL = 7.7 mm individual)
Colour of inhalant and exhalant regions	Dark yellow with opaque white spots	Fine opaque pinkish spots on pale or slightly brownish background	With fine opaque white spots	Fine, opaque white spots	Yellowish brown
Size of labial palps	A few folds per palp;16 folds per palp in 10 mm animal; between 9 and 16 folds per palp for SL range 8.0–12.5 mm animals (see Fig. 11)	Medium size, 20 folds per palp in 7 mm animal; outer palps generally larger than inner palps; number of folds variable (40 folds in 12 mm animal; see Fig. 11)	Large, 1/3 length of gills; 31 folds per palp in 7 mm animal; outer palps generally larger than inner palps; number of folds variable (57 folds in 12 mm animal; see Fig. 11)	Short, one-fifth length of gills, 18 folds per palp in 12 mm animal (see Fig. 11)	Short, one-fifth length of gills, 15 folds per palp in 7.7 mm individual
Size of anterior complex of byssus glands	Small and simple; condensed mass	Branching, deeply penetrating into visceral mass; condensed mass	Condensed mass above base of foot, not penetrating into visceral mass; condensed mass	Condensed mass	Condensed mass
Special byssus secretions (= byssal hairs) on shell	Absent	Usually conspicuous in small and medium-sized specimens; heavy and adhering, forming commarginal series of thickenings or blunt serrations	Weak or absent	Weak	Absent
Posterior adductor	Two unequal portions	Two markedly unequal portions	Two unequal portions	Two unequal portions	Two unequal portions
Posterior byssal retractors	Two main bundles; anterior bundle subdivided further into 2–3 bundles	Two main bundles	Two main bundles	Two main bundles	One main bundle

Table 1. Continued

Character	*Vignadula atrata*	*Vignadula balani*	*Vignadula mangle* comb. nov.	*Vignadula kuraburiensis* sp. nov.	*Xenostrobus pulex*
Plicate organ (= organ of Sabatier)	Absent	Present (inner and outer)	Present (inner and outer)	Absent	Present (outer only)
Egg diameter	?	45–50 µm	50 µm	?	58–68 µm for *Xenostrobus neozelanicus* (see Redfearn *et al.*, 1986)
Prodissoconch II	Small, convex, diameter 260 µm	Moderately convex, diameter 305–330 µm	Moderately convex, diameter 330–375 µm	Small, convex, diameter 210–230 µm	Diameter 300 µm

Text in blue is from Ockelmann (1983), text in red from Kimura (1996) and text in black from the present study. *Vignadula balani* and *V. mangle* comb. nov. are here regarded as synonyms (see main text).

Table 2. Major morphological traits that differentiate Xenostrobinae from mytilid genera currently placed in the Arcuatulinae (World Register of Marine Species, accessed 16 November 2021)

Trait	Xenostrobinae	*Limnoperna*	*Mytella*	*Arcuatula*
Teeth on inner margin of valves	No	No	Yes (anterior end only)	Yes (dorsal and anterior margins)
Resilium pits	No	No	Yes	No
Posterior byssal retractor muscle scars clearly separated?	No (Category 2 of Morton, 2015a)	Yes (Category 3)	No (Category 2)	Yes (Category 3)
Ctenidial attachment muscle scars	No	Yes (Morton & Dinesen, 2010)	No	No
Position of gut loop	Right of animal (Wilson, 1967; this study)	Left of animal (Kimura *et al.*, 1999)	Left of animal (Tan KS, pers. obs.)	Left of animal (pers. obs.)
Plicate gland (organ of Sabatier)	Absent in type species of *Xenostrobus* and *Vignadula*; present in some species (this study)	Present (outer) (Thomsen *et al.*, 2018)	Absent in *Mytella strigata* (Hanley, 1843) (Tan KS, pers. obs.)	Absent (Thomsen *et al.*, 2018 [as *Musculista*])

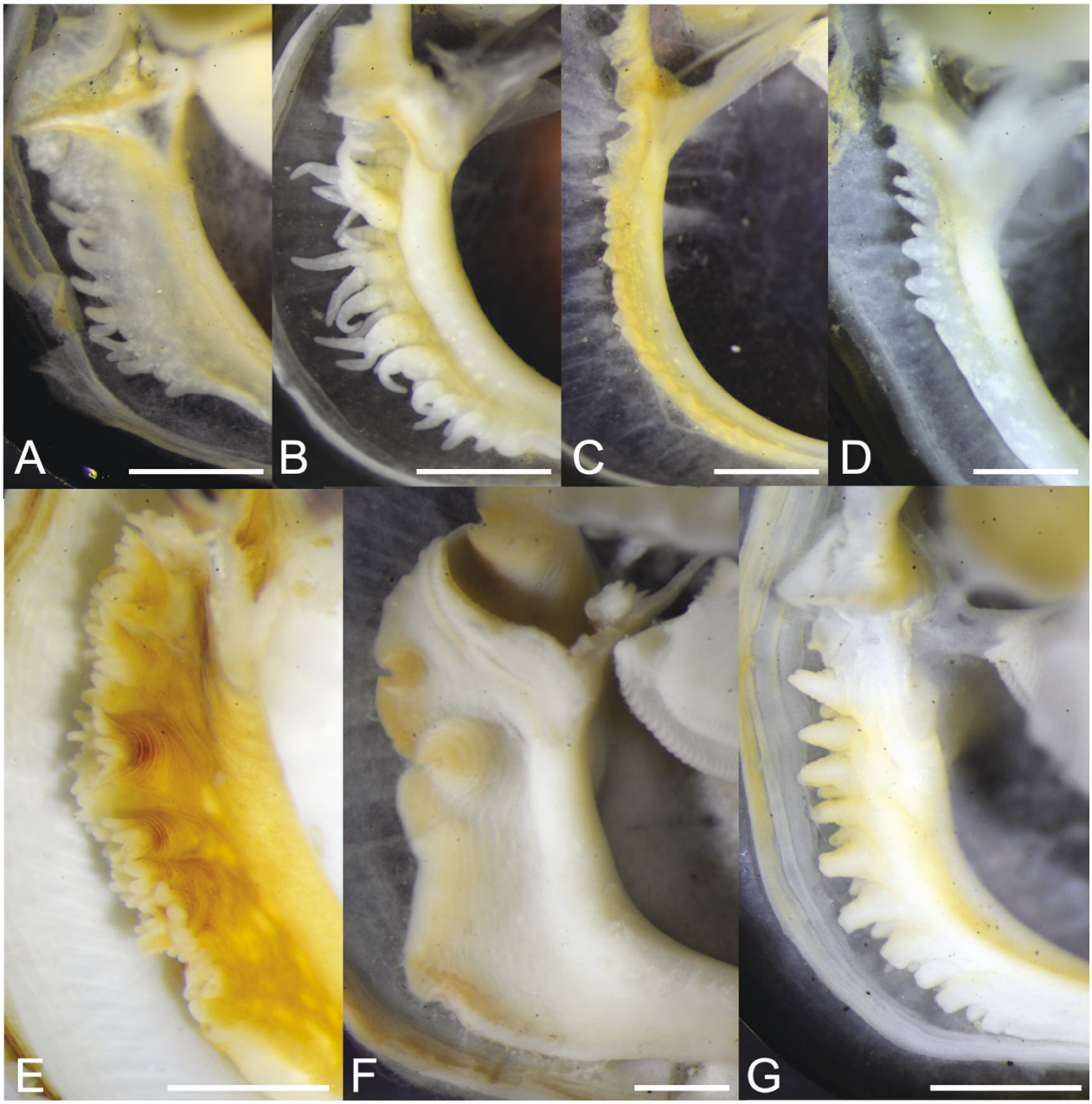

Figure 12. Guard papillae of *Vignadula* (A–D) and *Xenostrobus* (E–G) species on the posterior region of the inner mantle margin attached to LV. All animals shown preserved in ethanol. A, *Vignadula atrata*, SL = 11.4 mm, Toishi-ko, Nagasaki, Japan. B, *Vignadula mangle* comb. nov., SL = 13.5 mm, Kampong Bako, Kuching, Sarawak. C, *Vignadula kuraburiensis* sp. nov., SL = 13.2 mm, Kuraburi, Phangnga, Thailand. D, *V. kuraburiensis* sp. nov., SL = 8.8 mm, Ban Baen, Ranong, Thailand. E, *Xenostrobus inconstans*, SL = 22.7 mm, Dunnalley Bay, Tasmania, Australia (TMAG E21829). F, *Xenostrobus securis*, SL = 24.8 mm, Swan River, Perth, WA, Australia. G, *Xenostrobus pulex*, SL = 13.1 mm, Cottesloe, Perth, WA, Australia. Scale bars: 1 mm in A–C, E–G; 500 μm in D.

VIGNADULA KURABURIENSIS SP. NOV.

(FIGS 1–3, 7, 11, 12C, D, 13)

ZooBank registration.: urn:lsid:zoobank.org:act:F15E6689-04B3-43C6-B44E-7D98457FFB98

Diagnosis: Light brown to dark purple mytiliform shells with terminal umbones; anterior half of ventral region often golden yellow; animal without plicate gland; mantle edge at posterior region of animal bears ≤ 18 short, simple guard papillae.

Etymology: Named after the district of Kuraburi, Phang-nga Province in south-west Thailand, where the species was first collected. The gender of the genus *Vignadula* (Kuroda & Habe, 1971) was not given explicitly in the original description, but is here assumed to be female because the species name of the type species was changed from *atratus* to *atrata* (Kuroda *et al.*, 1971: 348, 549).

Material examined: Holotype: *PMBC 25290*, Ta Bon Bang Wan jetty south of the mouth of Baan Tang La Ong, Kuraburi District, Phang-nga Province, Thailand; SL = 12.8 mm (sequenced, XTSW1; Fig. 7A, B). Paratypes: PMBC 25291, SL = 13.2 mm (Fig. 7C, D); ZRC.MOL.24068, SL = 12.3 mm (sequenced, XTSW3; Fig. 7E, F); PMBC 25291 (sequenced, XTSW4); ZRC. MOL.24069, 24083 (intact individuals); Bang Ben Bay, Laem Son National Park, Ranong Province, Thailand, ZRC.MOL.24070 (sequenced, XTSW5), 24084 (intact individuals).

Shell: Length ≤ 15 mm, thin, outline mytiliform; anterior region narrow, umbones terminal, barely separated from anteroventral extension; posterior region expanded, flat. Surface light brown to dark purple over dorsal region and posterior two-thirds of length of valves, anteroventral region golden yellow. Valve surfaces with fine, closely set commarginal lines that may be outlined in a darker colour. 'Special byssal secretions' (*sensu* Ockelmann, 1983; i.e. commarginal thickenings or serrations, presumably secreted by the foot) may be present. Umbones and anteroventral margin are in line. Prodissoconch II diameter ~210–230 µm. Shell interior iridescent, usually reflecting the colour of the exterior; margins devoid of teeth. Ligament narrow, smooth without teeth; resilial pits absent.

Shell microstructure: Shell generally comprises two layers below the periostracum: a thin prismatic layer, under which a thick sheet nacreous layer is present. A thin, fibrous prismatic myostracum may be present within the sheet nacreous layer.

Anatomy: Up to 18 short, simple guard papillae along each side of inner mantle edge forming the inhalant aperture. Papillae translucent white, with opaque white subcutaneous pigment. Posterior byssal retractor muscles are split into two bundles (as observed on animal, although the muscle scars on the valves do not reflect this separation). Pericardium lies anterior to the posterior byssal retractor muscle complex (Category 2 of Morton, 2015a). Plicate organ absent. Foot yellowish white, vermiform. Labial palps vary in length according to shell size (see Theisen, 1982; Ockelmann, 1983), as does the number of folds (sorting ridges), which can range between 18 and 24 for SLs 10–13 mm (Fig. 11).

Habitat: Mid- to high intertidal, amongst oysters (*Saccostrea* Dollfus & Dautzenberg, 1920) on concrete pilings under jetty near mangroves.

Geographical distribution (Fig. 13): So far, found only in Phang-nga and Ranong provinces along the Andaman Sea coast of Thailand.

Similar species: Owing to the inherent variability of shell outline and colour in *V. atrata* and *V. mangle* (see Figs 4–6), it is generally difficult to separate the new species from its congeners based solely on external appearance. However, in anatomical terms *V. kuraburiensis* is distinguished from *V. mangle* in having fewer folds on its labial palps (< 20 folds in an animal ~12–14 mm SL; see Fig. 11) in comparison to the more numerous (> 30 folds) labial palp folds in *V. mangle* (Table 1). In addition, the absence of a plicate organ (organ of Sabatier; Thomsen *et al.*, 2018) at the base of the ctenidium in the new species also clearly distinguishes it from *V. mangle*. As for *V. atrata*, it is anatomically similar to *V. kuraburiensis* (i.e. small labial palps and absence of plicate glands), and although the two species are genetically distinct and do not overlap in geographical distribution, they cannot be separated reliably using external or internal morphology.

DISCUSSION

Our phylogenetic analysis of small, black mussel species from Southeast Asia based on nuclear and mitochondrial genes revealed their close relationship with *Xenostrobus* species distributed in Australia and New Zealand. All species share a unique anatomical feature in having their intestine loop on the right side of the animal (Wilson, 1967; Ockelmann, 1983; Kimura, 1996; Kimura *et al.*, 1999). Considered together with their similar shell morphology and comparable habitats in which they occur, the assignment of Southeast Asian species to the genus *Xenostrobus* was easily accepted in the absence of molecular evidence. However, our phylogenetic study revealed that they clearly comprised two sister clades that are each well supported based on BI and ML analyses of gene sequences. One clade is made up exclusively of species distributed natively in Australia and New Zealand: *X. inconstans*, *Xenostrobus neozelanicus* (Iredale, 1915), *X. pulex* and *X. securis*, while the other clade consists only of East and Southeast Asian species: *V. atrata*, *V. mangle* (= *V. balani*) and *V. kuraburiensis*. Given their close genetic and distinct geographical

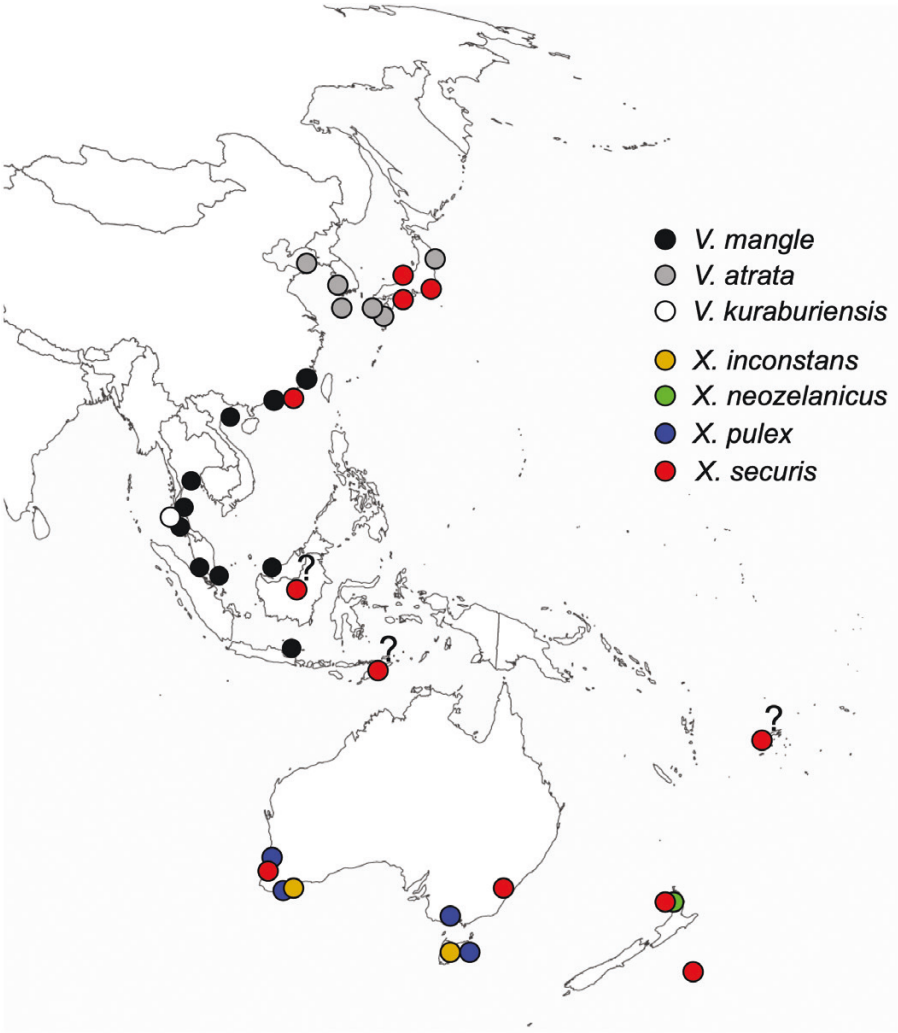

Figure 13. Geographical distribution of *Vignadula* and *Xenostrobus* species in East Asia, Australia and New Zealand. Locations are based on examined museum material or material collected in the field for this study by the authors, and supplemented by information contained in papers by Colgan (2017: *Xenostrobus securis*); Colgan *et al.* (2020: *Xenostrobus neozelanicus* and *X. securis*); Horikoshi & Okamoto (2007: *X. securis*); Iwasaki (2013: *X. securis*); Iwasaki & Yamamoto (2014: *X. securis*); Kimura (1996: *Vignadula atrata*); Kimura *et al.* (1999: *X. securis* [?], as *Xenostrobus* sp.); Lee & Morton (1985: *Vignadula mangle* comb. nov., as *Xenostrobus atratus*); Lamarck (1819: *X. securis* [?], as *Mytilus securis*; MNHN-IM-2000-34894, three syntypes); Lutaenko *et al.* (2019: *V. atrata*); Morton (1999: *Xenostrobus pulex*); Morton (2004: *Xenostrobus inconstans*); Morton & Leung (2015: *X. securis*); Park *et al.* (2017: *V. atrata*); Wang *et al.* (2011: *V. atrata*); Wilson (1967: *Xenostrobus* spp.).

distributions, we propose here to retain only the Australian and New Zealand species in the genus *Xenostrobus* and resurrect the available genus taxon *Vignadula* for the East and Southeast Asian species.

The appreciable support of the (*Xenostrobus* + *Vignadula*) clade in the concatenated trees (see Figs 1–3) and its close affinity to Modiolinae and Bathymodiolinae are also interesting. Although previous studies on Mytilidae using concatenated datasets have been unable to resolve the position of *Bathymodiolus* Kenk & B. R. Wilson, 1985 relative to *Xenostrobus* with high support (Kartavtsev et al., 2018, Audino *et al.*, 2020, Morton *et al.*, 2020a, b), our study shows *Modiolus* and *Bathymodiolus* to form a distinct clade, likewise for *Vignadula* and *Xenostrobus*. The distinctive anatomical synapomorphy in the position of the gut loop on the right side of the animal in members of *Vignadula* and *Xenostrobus* warrants their recognition as a separate subfamily, although relationships of mytilids at subfamily and genus levels are still uncertain (Wilson, 2006; Liu *et al.*, 2018). However, as pointed out by Liu *et al.*

(2018), Lee *et al.* (2019) and Morton *et al.* (2020a, b), the presence of two clades of Mytilidae (Clades 1 and 2 in the studies by Liu *et al.*, 2018 and Lee *et al.*, 2019; Clades A and B in the studies by Morton *et al.*, 2020a, b) is strongly supported, with *Xenostrobus*, *Vignadula*, *Modiolus*, *Bathymodiolus*, *Idas* Jeffreys, 1876, *Leiosolenus* Carpenter, 1857, *Limnoperna* and *Sinomytilus* Thiele, 1934 belonging to Clade 1 (Fig. 3, this study; Clade A of Morton *et al.*, 2020a; Clade B of Morton *et al.*, 2020b). Likewise, the current formal position of *Xenostrobus* in the subfamily Arcuatulinae (Scarlato & Starobogatov, 1979) is unsupported in all scenarios. *Xenostrobus* (and implicitly, *Vignadula*) is currently placed in Arcuatulinae (see World Register of Marine Species; accessed 16 November 2021) together with *Limnoperna*, *Mytella* Soot-Ryen, 1955 and *Arcuatula* Jousseaume in Lamy, 1919, but this arrangement appears not to be consistent with their morphology (see Table 2) or phylogenetic relationships (see also Morton *et al.*, 2020a: 127).

This study also points to the presence of at least three *Vignadula* species in East Asia, based on genetic and morphological evidence: *V. atrata*, ranging from Korea, north-east China and southern Japan in north-east Asia; *V. mangle* (shown here to be synonymous with *V. balani*), with a widespread distribution from Kinmen in Taiwan southwards to Thailand, Malaysia, Singapore and Java; and the newly described *V. kuraburiensis*, so far known only from the Andaman Sea coast of Thailand. The three species are externally similar (see Figs 4–7, 9). All are small, not exceeding 15 mm, with shells that are purplish black to dark brown/yellow in overall colouration. They occur byssately attached in and amongst barnacles and oysters in the mid- to upper intertidal zone, most often associated with areas influenced by estuarine conditions. Anatomically, they all possess guard papillae along the inner mantle lobe forming the inhalant siphon. These papillae can be simple or branched, and the number of papillae generally increases with shell size. In addition, their posterior byssal retractor muscles are formed from two bundles partly fused together. The specimens from Kinmen in Taiwan, for which only the shorter mt-*COI* barcode was available, were resolved as being closely related to Southeast Asian *V. mangle* and might represent a subspecies or a closely related cryptic species. Although anatomically indistinguishable from the Southeast Asian clade, genetic distances between the clades (0.1251 for mt-*COI*) exceed most accepted definitions of interspecific *COI* differences. At the same time, thresholds for determining species must be taken with caution, given that such a value is still markedly lower than that between other anatomically distinct *Vignadula* species, and for *Xenostrobus* species also. The use of the shorter mt-*COI* barcode might have led to the relatively greater value of genetic distance between the clades. Here, we regard the Taiwanese specimens as *V. mangle*.

The three species differ from each other morphologically in a few subtle aspects. In terms of their external appearance, *V. atrata* and *V. kuraburiensis* both have a typical mytiloid shell outline with generally terminal umbones, whereas the shell of *V. mangle* is trapezoid in outline, having a blunt but prominent anterior region, with generally subterminal umbones, and an obtusely angled dorsoposterior region. Internally, the labial palps of *V. atrata* and *V. kuraburiensis* possess fewer folds than *V. mangle* (Fig. 11). The plicate gland (organ of Sabatier; also osphradium) is absent in *V. atrata* and *V. kuraburiensis*, but present in *V. mangle*. Thus, *V. atrata* and *V. kuraburiensis* are more similar anatomically in comparison to *V. mangle*, having shared features such as an absent plicate organ, but have not been shown to form a clade in any dataset. Given that the plicate organ is present in *X. securis* (Thomsen *et al.*, 2018) and *X. pulex* (Table 1), it is possible that this trait was lost in the common ancestor of *Vignadula* and regained in an ancestor of *V. mangle*.

As shown in our phylogenetic trees, the closest genetic relatives of *Vignadula* outside East and Southeast Asia belong to the genus *Xenostrobus*. Two species, *X. pulex* and *X. neozelanicus*, are found in southern Australia and New Zealand, respectively (Colgan *et al.*, 2020). Although previously considered to be synonymous in view of their similar shells, they were recently shown to be sufficiently distinct genetically to be considered as separate species (Colgan & da Costa, 2013; Colgan *et al.*, 2020). Both species can attain SLs > 25 mm (Wells & Bryce, 1988; Tan KS, pers. obs.) and have dark, purplish black mytiloid shells with terminal umbones. We were unable to examine the anatomy of *X. neozelanicus*, but in *X. pulex* numerous simple and profusely branched guard papillae are present (Wilson, 1967: fig. 2c; up to ten branches on each papilla can be observed: Tan KS, pers. obs.; see also Fig. 12G). Labial palps are small, with few folds, and an outer plicate gland is present. Its relationship with *X. inconstans*, the type species of *Xenostrobus*, is currently unresolved. The molecular signatures of the two species are indistinct and possibly conspecific (Colgan & da Costa, 2013), but the shells of *X. pulex* and *X. inconstans* are clearly different (relatively thick shelled and dark purple in the smaller *X. pulex*, compared with the thin-shelled valves that are usually coloured light and dark brown for the larger *X. inconstans*; see also descriptions by Wilson, 1967). Internally, neither an outer nor inner plicate gland occurs in *X. inconstans* (Tan KS, pers. obs.), whereas the outer plicate gland is present in *X. pulex*, at least for those occurring in the vicinity of Perth, WA, Australia. The posterior byssus retractor muscle bundles are in two bundles (although

not apparent in the muscle scars of the valves) in *X. inconstans* as opposed to one in *X. pulex*. In addition, *X. pulex* generally inhabit rocky shores (Morton, 1999), whereas *X. inconstans* often occur amongst seagrass and sedges in marshes (Morton, 2004).

Xenostrobus securis is the only species in the genus to be distributed across Australia and New Zealand (Wilson, 1967; Wells, 1984). However, Lamarck (1819) described *X. securis* based on material from Australia and Timor. Wilson (1967) believed the latter locality to be in error, but there is one unregistered lot of three specimens (SL = 26–29 mm) in the Natural History Museum, London with an accompanying label '*Modiolus sinensis* Heude' from Borneo, which appear to be *X. securis* (Tan KS, pers. obs.). Wilson had previously examined these specimens and concluded in an accompanying handwritten note that they were *X. securis* but believed the locality was again erroneous. In addition, Kimura *et al.* (1999: 110, pl. 1 fig. 5) examined two specimens from Suva Point, Fiji that were identified as '*Xenostrobus* sp.' but remarked that they '…were similar anatomically and morphologically to *X. securis*'. Regardless of its original distribution, it is now established in Japan (Kimura *et al.*, 1999) and Hong Kong (Morton & Leung, 2015), in addition to the Mediterranean Sea and the Bay of Biscay in the Atlantic Ocean (Colgan, 2017 and references therein). Simple, unbranched tapering byssal hairs, which are flattened in cross-section, can be observed attached to the valve surfaces of smaller individuals (Ockelmann, 1983; Tan KS, pers. obs.). Posterior mantle guard papillae are entirely lacking (Fig. 12F; i.e. the edge of the posterior region of the inner mantle margin is smooth, without papillae). An outer plicate gland occurs in *X. securis*. These traits, in addition to its phylogenetic position as sister to other *Xenostrobus* species (see Figs 1–3), seem to suggest its relative separation from its congeners.

Ockelmann (1983) considered *Mytilus hepaticus* Gould, 1850 described from the Fiji Islands (see Gould, 1852: 454 and pl. 41, fig. 563; Kimura *et al.*, 1999: pl. 1, fig. 6) to be a *Xenostrobus*, but current opinion (World Register of Marine Species, accessed 16 November 2021) regards Gould's species as a junior synonym of the South African *Modiolus auriculatus* (Krauss, 1848). The absence of papillae on its inner mantle lobes was observed by Ockelmann (1983), but this is also true for many *Modiolus* species and for *X. securis*.

The taxonomic status of *Modiola sambasensis* Dautzenberg, 1904 (Fig. 14A, B), described from the estuary of the Sambas River, north-west Borneo (in present-day Kalimantan, Indonesia), remains unclear. Ockelmann (1983) considered this species to belong to *Xenostrobus*. We were unable to obtain living or preserved specimens for observation, and no molecular sequences corresponding to this species are currently available on GenBank. However, based on an examination of the valves of the holotype specimen (Fig. 14A, B), we suggest here that it is probably allied to *Limnoperna*, considering its sharp, angular dorsal outline and pronounced lateral keel. The presence of a second posterior byssal retractor muscle scar and a linear series of ctenidial attachment muscle scars (Fig. 14; see also Morton & Dinesen, 2010; Morton, 2015b; Sokolova *et al.*, 2021) on the inside surface of the valves is also reminiscent of *Limnoperna*. Although such scars are not restricted to *Limnoperna* [see e.g. Dinesen & Morton (2014) for *Modiolus modiolus* (Linnaeus, 1758)], they are absent in *Vignadula* and *Xenostrobus*. Likewise, *Modiolus taprobanensis* Preston, 1915 (Fig. 14C–H) is another species with valves that lack teeth along its margins, and bear a superficial resemblance to *Xenostrobus* and *Vignadula* species in outline. However, a second posterior byssal retractor muscle scar and a linear series of ctenidial attachment muscle scars are present, as observed in *Limnoperna*. Thus, this mussel from Sri Lanka (type locality; also recorded by Preston, 1916: 35 from Ennur backwater, Madras, but see Tan *et al.*, 2021: 95) could again be related more closely to *Limnoperna* than to *Vignadula* or *Xenostrobus* (however, see Morton & Dinesen, 2010, who attributed *Modiolus taprobanensis* to either *Musculista* Yamamoto & Habe, 1958 or *Brachidontes* Swainson, 1840, whereas Sokolova *et al.*, 2021: 1181 suggested *Modiolus taprobanensis* to be a marine species). These hypotheses await further study.

Conclusion

Mussels characterized by having their intestine looped on their right side are common on the intertidal seashores in the vicinity of estuaries in East Asia and Australasia. Genetic evidence suggests that they form a monophyletic group (herein assigned to the new subfamily Xenostrobinae) whose immediate sister clades are Modiolinae and deep-sea Bathymodiolinae. The xenostrobines, in turn, comprise two genera, *Xenostrobus* and *Vignadula*. Members of *Xenostrobus* appear to be confined to temperate Australia and New Zealand (although records of *X. securis* from Timor, Borneo and Fiji require confirmation), whereas those of *Vignadula* are generally smaller in size and distributed in East and Southeast Asia. Three species are assigned to the latter genus. The type species of the genus, *V. atrata*, occurs in temperate north-east Asia. The second species, *V. mangle* (including its synonym *V. balani*), is widely distributed in Southeast Asia and southern China. The third species, *V. kuraburiensis*, is described as a new species and is currently known only from the Andaman Sea coast of Thailand. All three *Vignadula* species have shells that are remarkably similar in shape and size. At the same time, those of *V. atrata* and *V. mangle* are variable in outline,

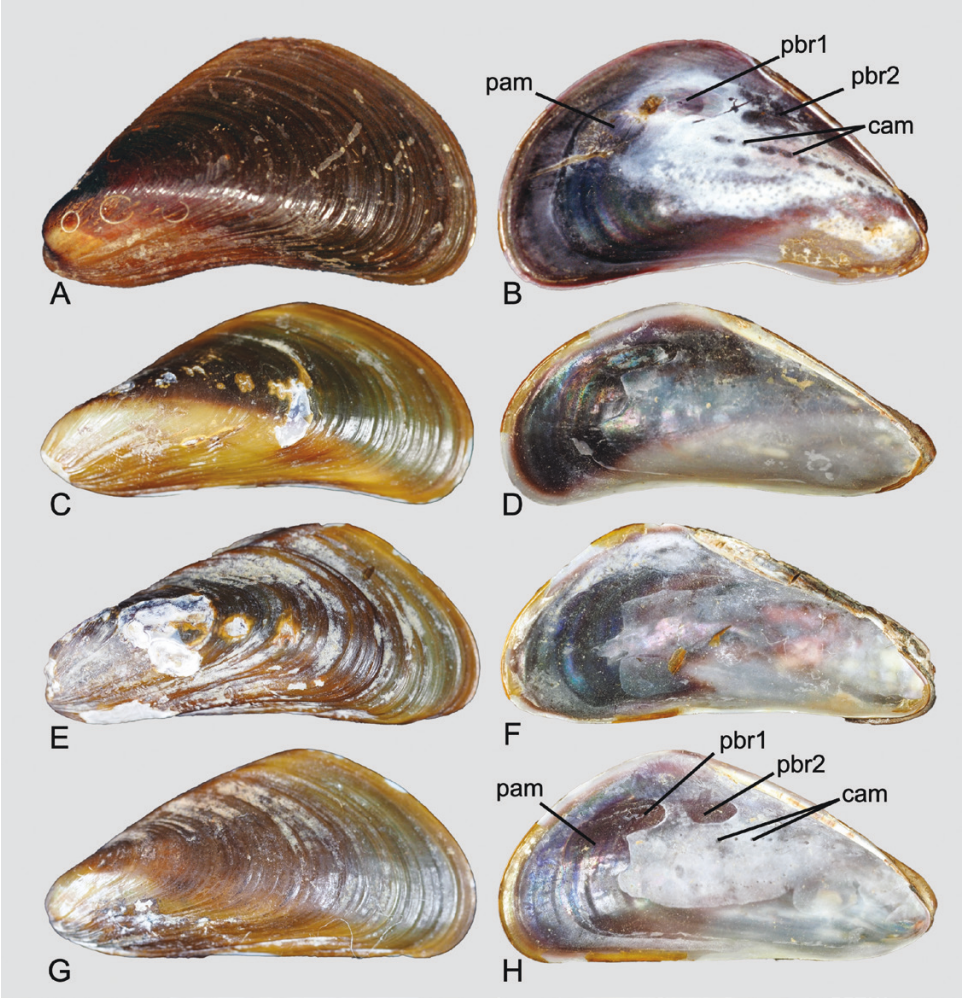

Figure 14. Type material of species that are more aligned to *Limnoperna* than to *Xenostrobus* or *Vignadula*. A, B, holotype of *Modiolus sambasensis* Dautzenberg, 1904 from Sambas River, Kalimantan, north-west Borneo (IRSN); SL = 16.2 mm. C–H, syntypes of *Modiolus taprobanensis* Preston, 1915 from Ceylon (Sri Lanka) (BMNH). C, D, SL = 17.5 mm. E, F, SL = 18.6 mm. G, H, SL = 18.5 mm. Abbreviations: cam, ctenidial attachment muscle scar; pam, posterior adductor muscle; pbr1, first posterior byssal retractor muscle; pbr2, second posterior byssal retractor muscle.

which has given rise to much confusion. Although they are clearly distinct genetically, anatomical traits pertaining to the size of guard papillae, number of labial palp folds and presence or absence of plicate glands are useful in distinguishing the three species.

ACKNOWLEDGEMENTS

We express our sincere appreciation to the following curators for access to museum collections in their care: Thierry Backeljau (Institut Royal des Sciences Naturelles de Belgique, Brussels); Toshihiko Fujita and Hiroshi Saito (National Museum of Nature and Science, Tsukuba); Virginie Heros (Muséum nationale de Histoire naturelle, Paris); Charatsee Aungtonya (Phuket Marine Biological Center, Thailand); Lisa Kirkendale (Western Australian Museum, Perth); Tan Siong Kiat (Lee Kong Chian Natural History Museum, National University of Singapore); Tom White (Natural History Museum, London); and Lee Kun-Hsuan and Hung He-Tian (National Museum of Natural Science, Taichung). Elsewhere and in the field, Jaruwat Nabhitabhata (Prince of Songkhla University, Thailand), Fred Wells (Curtin University, Perth, WA, Australia), Liu Li-lian, Kang Dun-ru, Kuo Mong-ying and Wu Jingying (National Sun Yat-sen University, Kaohsiung, Taiwan) provided help and support. Simon Grove (Tasmanian Museum and Art Gallery, Hobart, TAS, Australia) kindly loaned specimens of *Xenostrobus inconstans* at short notice. Other *Xenostrobus* species were collected in the vicinity of

Perth, WA, Australia under permit application no. r1112435/exemption no. 3234. Helpful comments from two anonymous referees improved the manuscript. We are also grateful for the generous funding and support provided by the National Research Foundation, Prime MInister's Office, Singapore through the Marine Science Research and Development Programme (MSRDP). Travel expenses to examine material in the National Museum of Nature and Science, Tsukuba, Japan were generously supported by a grant from its Director General to Toshihiko Fujita. This study is an output of the MSRDP project entitled 'Biodiversity of mussels in Southeast Asia' (project P25). The authors declare no conflicts of interest.

DATA AVAILABILITY

Xenostrobine sequence data utilised in this article are available from the GenBank Nucleotide Database at https://www.ncbi.nlm.nih.gov/genbank/ and can be accessed with the following GenBank accession numbers: OL693326–OL693337; OL693339–OL693359; OL693361–OL693407; OL693410, OL693411; OL775461–OL775531; OL780612–OL780686; MW295361.1, OL780690–OL780760; OL804016, OL804017, OL813811–OL813814.

REFERENCES

Alves FAS, **Beasley CR**, **Hoeh WR**, **Rocha RM**, **Simone LRL**, **Tagliaro CH. 2012.** Detection of mitochondrial heteroplasmy suggests a double uniparental inheritance pattern in the mussel *Mytella charruana*. *Revista Brasileira de Biociências* **10:** 176–185.

Audino JA, **Serb JM**, **Marian JEAR. 2020.** Phylogeny and anatomy of marine mussels (Bivalvia: Mytilidae) reveal convergent evolution of siphon traits. *Zoological Journal of the Linnean Society* **190:** 592–612.

Aungtonya C, **Thaiklang N**, **Srisuwan D. 1999.** Recent records of Bivalvia in the reference collection of Phuket Marine Biological Center, Thailand. *Phuket Marine Biological Center Special Publication* **19:** 371–383.

Bernard FR, **Cai Y-Y**, **Morton B. 1993.** *Catalogue of the living marine bivalves of China*. Hong Kong: Hong Kong University Press.

Beu AG. 2006. Marine Mollusca of oxygen isotope stages of the last 2 million years in New Zealand. Part 2. Biostratigraphically useful and new Pliocene to Recent bivalves. *Journal of the Royal Society of New Zealand* **36:** 151–338.

Beu AG. 2012. Marine Mollusca of the last 2 million years in New Zealand. Part 5. Summary. *Journal of the Royal Society of New Zealand* **42:** 1–47.

Carter JG. 1990. Shell microstructural data for the Bivalvia. Part I. Introduction. In: Carter JG, ed. *Skeletal biomineralization: patterns, processes, and evolutionary trends, Vol. 1.* New York: Van Nostrand Reinhold, 297–301.

Colgan DJ. 2017. Fine-scale spatial partitioning of genetic variation and evolutionary contestability in the invasive estuarine mussel *Xenostrobus securis*. *Marine Biology Research* **13:** 1059–1072.

Colgan DJ, **da Costa P. 2013.** Invasive and non-invasive lineages in *Xenostrobus* (Bivalvia: Mytilidae). *Molluscan Research* **33:** 272–280.

Colgan DJ, **Hutchings PA**, **Brown S. 2001.** Phylogenetic relationships within the Terebellomorpha. *Journal of the Marine Biological Association of the UK* **81:** 765–773.

Colgan DJ, **Ponder WF**, **Beacham E**, **Macaranas JM. 2003.** Gastropod phylogeny based on six segments from four genes representing coding or non-coding and mitochondrial or nuclear DNA. *Molluscan Research* **23:** 123–148.

Colgan DJ, **Willan RC**, **Kirkendale LA. 2020.** A genetic assessment of the taxonomic status of New Zealand mussels of the genus *Xenostrobus* Wilson, 1967. *New Zealand Journal of Marine and Freshwater Research* **54:** 271–285.

Dall WH. 1871. Descriptions of sixty new forms of mollusks from the west coast of North America and the North Pacific Ocean, with notes on others already described. *American Journal of Conchology* **7:** 93–160, pls 13–16.

Dinesen GE, **Morton B. 2014.** Review of the functional morphology, biology and perturbation impacts on the boreal, habitat-forming horse mussel *Modiolus modiolus* (Bivalvia: Mytilidae: Modiolinae). *Marine Biology Research* **10:** 845–870.

Folmer O, **Black M**, **Hoeh W**, **Lutz R**, **Vrijenhoek R. 1994.** DNA primers for amplification of mitochondrial cytochrome *c* oxidase subunit I from diverse metazoan invertebrates. *Molecular Marine Biology and Biotechnology* **3:** 294–299.

Garrido-Ramos MA, **Stewart DT**, **Sutherland B**, **Zouros E. 1998.** The distribution of male-transmitted and female-transmitted mitochondrial DNA types in somatic tissues of blue mussels: implications for the operation of doubly uniparental inheritance of mitochondrial DNA. *Genome* **41:** 818–824.

Gould AA. 1852. *United States exploring expedition. During the years 1838, 1839, 1840, 1841, 1842. Under the command of Charles Wilkes, U.S.N. Vol. XII. Mollusca & Shells*. Boston: Gould & Lincoln.

Habe T. 1968. *Shells of the western Pacific in color, Vol. II*. Osaka: Hoikusha Publishing.

Habe T. 1981. A catalogue of molluscs of Wakayama Prefecture, the Province of Kii. 1. Bivalvia, Scaphopoda and Cephalopoda. *Publications of the Seto Marine Biological Laboratory, Special Series* **7:** xiii–xx, 15–264.

Habe T, **Kosuge S. 1967.** *Common shells of Japan in color*. Osaka: Hoikusha Publishing.

Horikoshi A, **Okamoto K. 2007.** Present sessile organism community structure on the intertidal coast of Tokyo Bay. *Sessile Organisms* **24:** 9–19.

Huber M. 2010. *Compendium of bivalves*. Hakenheim: Conchbooks.

Huelsenbeck JP, **Ronquist F. 2001.** MRBAYES: Bayesian inference of phylogenetic trees. *Bioinformatics* **17:** 754–755.

Iwasaki K. 2013. Distribution of the non-indigenous mytilid bivalve *Xenostrobus securis* along the Sea of Japan's Japanese coastline. *Japanese Journal of Benthology* **67:** 73–81.

Iwasaki K, **Yamamoto H. 2014.** Recruitment and population structure of the non-indigenous brackish water mytilid *Xenostrobus securis* (Lamarck, 1819) in the Kino River, Japan. *Aquatic Invasions* **9:** 479–487.

Kartavtsev YP, **Sharina SN**, **Chichvarkhin AY**, **Chichvarkhina OV**, **Masalkova NA**, **Lutaenko KA**, **Oliveira C. 2018.** Genetic divergence of mussels (Mollusca, Mytilidae) based on the *28S* rRNA, *18S* rRNA, and *H3* nuclear gene sequences. *Russian Journal of Genetics* **54:** 652–669.

Kimura T. 1996. Shell morphology and anatomy of *Xenostrobus atratus* (Lischke, 1871) (Bivalvia: Mytilidae). *Yuriyagai* **4:** 97–101.

Kimura T, **Tabe M**, **Shikano Y. 1999.** *Limnoperna fortunei kikuchii* Habe, 1981 (Bivalvia: Mytilidae) is a synonym of *Xenostrobus securis* (Lamarck, 1819): introduction into Japan from Australia and/or New Zealand. *Venus* **58:** 101–117.

Kumar S, **Stecher G**, **Li M**, **Knyaz C**, **Tamura K. 2018.** MEGA X: molecular evolutionary genetics analysis across computing platforms. *Molecular Biology and Evolution* **35:** 1547–1549.

Kuroda T. 1932. Japanese shells: Mytilidae (Appendix). *Venus* **3:** 123–134.

Kuroda T, **Habe T**, **Oyama K. 1971.** *The sea shells of Sagami Bay. Collected by His Majesty the Emperor of Japan*. Tokyo: Maruzen.

Kurozumi T. 2000. Family Mytilidae. In: Okutani T, ed. *Marine mollusks of Japan*. Kanagawa: Tokai University Press.

Kurozumi T. 2017. Family Mytilidae. In: Okutani T, ed. *Marine mollusks of Japan*, *2nd edn*. Kanagawa: Tokai University Press.

Lamarck JBPA. 1819. *Histoire naturelle des animaux sans vertèbres. Suite des Conchifères, Vol. 6.* Paris: Verdière.

Larsson A. 2014. Aliview: a fast and lightweight alignment viewer and editor for large datasets. *Bioinformatics* **30:** 3276–3278.

Lee SY, **Morton B. 1985.** The Hong Kong Mytilidae. In: Morton B, Dudgeon D, eds. *The malacofauna of Hong Kong and southern China II. Proceedings of the Second International Workshop on the Malacofauna of Hong Kong and Southern China, Hong Kong, 6–24 April 1983, Vol. 1*. Hong Kong: Hong Kong University Press, 49–76.

Lee Y, **Kwak H**, **Shin J**, **Kim SC**, **Kim T**, **Park JK. 2019.** A mitochondrial genome phylogeny of Mytilidae (Bivalvia: Mytilida). *Molecular Phylogenetics and Evolution* **139**, 106533. https://doi.org/https://doi.org/10.1016/j.ympev.2019.106533

Leh MUC, **Sasekumar A**, **Chew LL. 2012.** Feeding biology of eel catfish *Plotosus canius* Hamilton in a Malaysian mangrove estuary and mudflat. *Raffles Bulletin of Zoology* **60:** 551–557.

Leray M, **Yang JY**, **Meyer CP**, **Mills SC**, **Agudelo N**, **Ranwez V**, **Boehm JT**, **Machida RJ. 2013.** A new versatile primer set targeting a short fragment of the mitochondrial COI region for metabarcoding metazoan diversity: application for characterizing coral reef fish gut contents. *Frontiers in Zoology* **10:** 34.

Lischke CE. 1871a. Diagnosen neuer Meeres-Conchylien von Japan. *Malakozoologische Blätter* **18:** 39–45.

Lischke CE. 1871b. *Japanische Meeres-Conchylien. Ein Beitrag zur Kenntnis der Mollusken Japan's, mit bersonderer Rücksicht auf die geographische Verbreitung derselben. II*. Kassel: Theodor Fischer.

Liu J, **Li Q**, **Kong LF**, **Chen J**, **Zheng XD**, **Yu RH. 2011.** COI-based DNA barcoding in Mytilidae species (Mollusca: Bivalvia). *Acta Hydrobiologica Sinica* **35:** 874–881.

Liu J, **Liu H**, **Zhang H. 2018.** Phylogeny and evolutionary radiation of the marine mussels (Bivalvia: Mytilidae) based on mitochondrial and nuclear genes. *Molecular Phylogenetics and Evolution* **126:** 233–240.

Lutaenko KA, **Chaban EM. 2016.** Bivalve collection of C. E. Lischke in the Zoological Institute, St. Petersburg: Mytilidae, Ungulinidae and Tellinidae. *Korean Journal of Malacology* **32:** 141–147.

Lutaenko KA, **Noseworthy RG**, **Choi K-S. 2019.** Marine bivalve mollusks of Jeju Island (Korea). Part 1. *Korean Journal of Malacology* **35:** 149–238.

MacArthur AG, **Koop BF. 1999.** Partial 28S rDNA sequences and the antiquity of hydrothermal vent endemic gastropods. *Molecular Phylogenetics and Evolution* **13:** 255–274.

Madin J, **Chong VC**, **Basri B. 2009.** Development and short-term dynamics of macrofouling assemblages on fish-cage nettings in a tropical estuary. *Estuarine, Coastal and Shelf Science* **83:** 19–29.

Morton B. 1999. Competitive grazers and the predatory whelk *Lepsiella flindersi* (Gastropoda: Muricidae) structure a mussel bed (*Xenostrobus pulex*) on a southwest Australian shore. *Journal of Molluscan Studies* **65:** 435–452.

Morton B. 2004. Predator-prey interactions between *Lepsiella vinosa* (Gastropoda: Muricidae) and *Xenostrobus inconstans* (Bivalvia: Mytilidae) in a southwest Australian marsh. *Journal of Molluscan Studies* **70:** 237–245.

Morton B. 2015a. Evolution and adaptive radiation in the Mytiloidea (Bivalvia): clues from the pericardial-posterior byssal retractor musculature complex. *Molluscan Research* **35:** 227–245.

Morton B. 2015b. The biology and anatomy of *Limnoperna fortunei*, a significant freshwater bioinvader: blueprints for success. In: Boltovskoy D, ed. Limnoperna fortunei, *Invading Nature. Springer Series in Invasion Ecology, 10*. Cham: Springer International Publishing, 3–41.

Morton B, **Dinesen GE. 2010.** Colonization of Asian freshwaters by the Mytilidae (Bivalvia): a comparison of *Sinomytilus harmandi* from the Tonle-Sap River, Phnom Penh, Cambodia with *Limnoperna fortunei*. *Molluscan Research* **30:** 57–72.

Morton B, **Leung KF. 2015.** Introduction of the alien *Xenostrobus securis* (Bivalvia: Mytilidae) into Hong Kong, China: interactions with and impacts upon native species and the earlier introduced *Mytilopsis sallei* (Bivalvia: Dreissenidae). *Marine Pollution Bulletin* **92:** 134–142.

Morton B, **Leung PTY**, **Wei J**, **Lee GY. 2020a.** Phylogenetic relationships of Asian freshwater Mytiloidea (Bivalvia): a morphological and genetic comparison of *Sinomytilus harmandi*, *Limnoperna fortunei* and *Septifer bilocularis*. *Molluscan Research* **40:** 120–129.

Morton B, **Leung PTY**, **Wei J**, **Lee GY. 2020b.** A morphological and genetic comparison of *Septifer bilocularis*, *Mytilisepta virgata* and *Brachidontes variabilis* (Bivalvia: Mytiloidea) from Hong Kong and erection of the Mytiliseptiferinae subfam. nov. *Regional Studies in Marine Science* **34:** 100981.

Ng PKL, **Sivasothi N. 1999.** *A guide to the mangroves of Singapore II (animal diversity)*. Singapore: Singapore Science Centre.

Nguyen C. 2001. Mytilidae (Mollusca: Bivalvia) recorded in Vietnam. *Phuket Marine Biological Center Special Publication* **25:** 411–417.

Nguyen LT, **Schmidt HA**, **von Haeseler A**, **Minh BQ. 2015.** IQ-TREE: a fast and effective stochastic algorithm for estimating maximum likelihood phylogenies. *Molecular Biology and Evolution* **32:** 268–274.

Ockelmann KW. 1983. Descriptions of mytilid species and definition of the Dacrydiinae n. subfam. (Mytilacea–Bivalvia). *Ophelia* **22:** 81–123.

Park C, **Kim S-T**, **Hong J-S**, **Choi K-H. 2017.** A rapid assessment survey of invasive species of macrobenthic invertebrates in Korean waters. *Ocean Science Journal* **52:** 387–395.

Pleyte K, **Duncan SD**, **Phillips RB. 1992.** Evolutionary relationships of the salmonid fish genus *Salvelinus* inferred from DNA sequences of the first internal transcribed spacer (ITS 1) of ribosomal DNA. *Molecular Phylogenetics and Evolution* **1:** 223–230.

Preston HB. 1916. Report on a collection of Mollusca from the Cochin and Ennur backwaters. *Records of the Indian Museum* **12:** 27–39.

Rafinesque CS. 1815. *Analyse de la Nature ou Tableau de l'Univers et des Corps organisés*. Palermo: (privately published).

Rambaut A. 2018. *FigTree*. Tree figure drawing tool. Available at: http://tree.bio.ed.ac.uk

Rambaut A, **Drummond AJ**, **Xie D**, **Baele G**, **Suchard MA. 2018.** Posterior summarization in Bayesian phylogenetics using Tracer 1.7. *Systematic Biology* **67:** 901–904.

Redfearn P, **Chanley P**, **Chanley M. 1986.** Larval shell development of four species of New Zealand mussels (Bivalvia, Mytilacea). *New Zealand Journal of Marine and Freshwater Research* **20:** 157–172.

Robicheau BM, **Powell AE**, **Del Bel L**, **Breton S**, **Stewart DT. 2016.** Evidence for extreme sequence divergence between the male- and female-transmitted mitochondrial genomes in the bivalve mollusc, *Modiolus modiolus* (Mytilidae). *Journal of Zoological Systematics and Evolutionary Research* **55:** 89–97.

Scarlato OA, **Starobogatov YI. 1979.** Osnovye cherty evoliutsii i sistema klassa Bivalvia [General evolutionary patterns and the system of the Class Bivalvia]. In: Starobogatov YI, ed. *Morfologiia, Sistematika i Filogeniia Molliuskov [Morphology, Systematics and Phylogeny of Mollusks]. Akademiia Nauuk SSSR, Trudy Zoologicheskogo Instituta* **80:** 5–38.

Sokolova AM, **Aksenova OV**, **Bespalaya YV**, **Goforov MY**, **Kondakov AV**, **Konopleva ES**, **Tomilova AA**, **Travina OV**, **Tanmuangpak K**, **Tumpeesuwan S**, **Vikhrev IV**, **Bolotov IN. 2021.** Integrative taxonomy and biogeographic affinities of the first freshwater sponge and mollusc association discovered in tropical Asia. *Journal of Zoological Systematics and Evolutionary Research* **59:** 1167–1189.

Tan KS, **Tan SHM**, **Sanpanich K**, **Duangdee T**, **Ambarwati R. 2021.** Taxonomic re-description and relationships of two mat-forming mussels from the Indo-Pacific region, with a proposed new genus. *Phuket Marine Biological Center Research Bulletin* **78:** 77–115.

Theisen BF. 1982. Variation in size of gills, labial palps, and adductor muscle in *Mytilus edulis* L. (Bivalvia) from Danish waters. *Ophelia* **21:** 49–63.

Thomsen J, **Morton B**, **Ossenbrügger H**, **Crooks JA**, **Valentich-Scott P**, **Haynert K. 2018.** The mytilid plicate organ: revisiting a neglected organ. *Journal of Molluscan Studies* **84:** 486–489.

Trifinopoulos J, **Nguyen LT**, **von Haeseler A**, **Minh BQ. 2016.** W-IQ-TREE: a fast online phylogenetic tool for maximum likelihood analysis. *Nucleic Acids Research* **44:** W232–W235.

Vaidya G, **Lohman DJ**, **Meier R. 2011.** SequenceMatrix: concatenation software for the fast assembly of multigene datasets with character set and codon information. *Cladistics* **27:** 171–180.

Wang X, **Sun H**, **Wang Y**, **Chang L**, **Yan D**, **Huang Q**, **Jing M. 2011.** *Common invertebrates of the Yantai seashore* [in Chinese]. Beijing: Science Press.

Wang Z. 1997. *Fauna Sinica. Phylum Mollusca, Order Mytiloida*. Beijing: Science Press.

Wang Z. 2004. Mytiloida. In: Qi Z, ed. *Seashells of China*. Beijing: China Ocean Press, 224–233, pls 118–123.

Wells FE. 1984. *A guide to the common molluscs of south-western Australian estuaries*. Perth: Western Australian Museum.

Wells FE, **Bryce CW. 1988.** *Seashells of Western Australia*. Perth: Western Australian Museum.

Wilson BR. 1967. A new generic name for three Recent and one fossil species of Mytilidae (Mollusca: Bivalvia) in southern Australasia, with redescriptions of the species. *Proceedings of the Malacological Society of London* **37:** 279–295.

Wilson BR. 2006. A new generic name for a burrowing mytilid (Mollusca: Bivalvia: Mytilidae). *Molluscan Research* **26:** 89–97.

SUPPORTING INFORMATION

Additional Supporting Information may be found in the online version of this article at the publisher's web-site:

Table S1. List of *Xenostrobus* (*s.l.*) specimen DNA codes used in Figures 1–3 for phylogenetic analyses, with corresponding localities, geographical coordinates, museum voucher specimen numbers and GenBank accession

numbers for mt-*COI*, ITS1, 28S D1R and *H3* genes. See also Figures 4–7 for images of shells of individuals from which tissue samples were obtained for DNA sequencing. Voucher specimens (valves and tissue) were deposited in the Zoological Reference Collection (ZRC), Lee Kong Chian Natural History Museum, National University of Singapore and the Phuket Marine Biological Center (PMBC) Reference Collection, Thailand. GenBank accession numbers marked with an asterisk (*) are 313 bp *COI* barcodes.

Table S2. Mytilid sequences obtained from GenBank (GB) based on previous studies (except for entries in grey, for which sequences were obtained in this study) that were used for phylogenetic analyses for Figures 1–3.

Table S3. Bootstrap estimates of average pairwise genetic distances between modioline/bathymodioline genera (clades BY and MD in Figs 2, 3) and the *Xenostrobus* clade (clade A + E in Fig. 2; Clade XS in Fig. 3) for the 313 bp fragment of *COI*, using 1000 replicates. Standard error rates are displayed after the genetic distance values. Intragenus genetic distances are displayed on the diagonal. Rate variation among sites was modelled as gamma distributed with invariant sites (G+I), with a gamma parameter of 1.00. All gaps in the alignment were deleted. For simplicity, only *Vignadula*, *Xenostrobus* and their closest relatives in Mytilidae Clade 1 (see Fig. 3) are included in this table.

Table S4. Bootstrap estimates of average pairwise genetic distances between modioline genera (clades BY and MD in Figs 2, 3) and the *Xenostrobus* clade (clade A + E, or *Xenostrobus* + *Vignadula* in Fig. 2; Clade XS in Fig. 3) for internal transcribed spacer 1, using 1000 replicates. *Bathymodiolus* was omitted owing to the lack of properly aligned representative sequences in databases.

Table S5. Bootstrap estimates of average pairwise genetic distances between modioline/bathymodioline genera (clades BY and MD in Figs 2, 3) and the *Xenostrobus* clade (clade A + E, or *Xenostrobus* + *Vignadula* in Fig. 2; Clade XS in Fig. 3) for the 28S D1R expansion region, using 1000 replicates.

Table S6. Bootstrap estimates of average pairwise genetic distance between modioline/bathymodioline genera (clades BY and MD in Figs 2, 3) and the *Xenostrobus* clade (clade A + E, or *Xenostrobus* + *Vignadula* in Fig. 2; Clade XS in Fig. 3) for *H3*, using 1000 replicates.

Table S7. Bootstrap estimates of average pairwise genetic distance ± SE between *Vignadula* and *Xenostrobus* taxa for the 313 bp fragment of *COI*, using 1000 replicates. Standard error rates are displayed after the genetic distance values. Intraspecies genetic distances are displayed on the diagonal. Rate variation among sites was modelled as gamma distributed with invariant sites, with a gamma parameter of 1.00. All gaps in the alignment were deleted. For simplicity, only species within *Xenostrobus* and putative (sub)species within *Vignadula* are included in this table.

Table S8. Bootstrap estimates of average pairwise genetic distance ± SE between *Vignadula* and *Xenostrobus* taxa for internal transcribed spacer 1, using 1000 replicates.

Table S9. Bootstrap estimates of average pairwise genetic distance ± SE between *Vignadula* and *Xenostrobus* taxa for the 28S D1R expansion region, using 1000 replicates. Note the lack of intraspecific variation within putative species, and between congeners *Xenostrobus securis* and *Xenostrobus pulex*. Abbreviations: SEA, Southeast Asia; TW, Taiwan.

Table S10. Bootstrap estimates of average pairwise genetic distance ± SE between *Vignadula* and *Xenostrobus* taxa for *H3*, using 1000 replicates. Note the lack of intraspecific variation within putative species. Abbreviations: SEA, Southeast Asia; TW, Taiwan.